UNIQA: UNIFIED VISION-LANGUAGE PRE-TRAINING FOR IMAGE QUALITY AND AESTHETIC ASSESSMENT

Anonymous authors
Paper under double-blind review

ABSTRACT

Image Quality Assessment (IQA) and Image Aesthetic Assessment (IAA) aim to simulate human subjective perception of image visual quality and aesthetic appeal. Despite distinct learning objectives, they have underlying interconnectedness due to consistent human assessment perception. Existing unified methods typically combine datasets of two tasks for regression training directly, which fail to learn mutually beneficial representations shared by both tasks explicitly. To confront this challenge, we propose **Uni**fied vision-language pre-training of **Q**uality and **A**esthetics (**UniQA**), to extract useful and common representations from two tasks, thereby benefiting them simultaneously. Unfortunately, the lack of text in the IQA datasets and the textual noise in the IAA datasets pose severe challenges for multimodal pre-training. To address this, we (1) utilize multimodal large language models (MLLMs) to generate high-quality text descriptions; (2) use the generated text for IAA as metadata to purify noisy IAA data. To effectively adapt the pre-trained UniQA to downstream tasks, we further propose a lightweight adapter that utilizes versatile cues to fully exploit the extensive knowledge of the pre-trained model. Extensive experiments show that our approach achieves state-of-the-art performance on both IQA and IAA tasks, while also demonstrating exceptional few-label image assessment capabilities.

1 INTRODUCTION

Image Quality Assessment (IQA)[1] and Image Aesthetic Assessment (IAA) aim to measure the perceived quality and beauty of an image. They find broad applications in many scenarios, such as guiding individuals in image photography and editing, and serving as tools for image dehazing model (Zhao et al., 2021). Consequently, huge efforts (Su et al., 2020; Ke et al., 2021; He et al., 2022) have been devoted to establishing effective IQA and IAA models.

IQA and IAA concentrate on distinct aspects of image assessment, with IQA primarily focusing on the distortion level of the image, while IAA is oriented towards evaluating the aesthetic appeal of the image. Despite their differences, IQA and IAA have underlying commonality: **simulating human subjective perceptions of images.** Specifically, in human subjective evaluation of images, quality and aesthetics exhibit a mutual influence, such that high-quality images are more likely to possess a higher aesthetic appeal compared to their low-quality counterparts. Thus, the learning process for both tasks not only acquires features unique to themselves but also involves the learning of task-agnostic common representations. This commonality sparks an idea:

> *Can we develop a foundational model with robust visual assessment perceptions consistent with human to benefit both IQA and IAA tasks?*

Although previous works (*e.g.*, MUSIQ (Ke et al., 2021)) can be applied to IQA and IAA tasks indiscriminately, they cannot exploit beneficial representations from another task. Wu et al. (2023b) and Zhang et al. (2023a) also find the similarities of two tasks and attempt to tackle them with unified architecture and training. However, they typically unify datasets of two tasks for regression training directly, which cannot explicitly learn the task-shared representations, restricting the extraction of mutual benefits. In this paper, we propose the **Uni**fied pre-training of **Q**uality and **A**esthetics

[1]The IQA in this work refers to the no-reference image quality assessment.

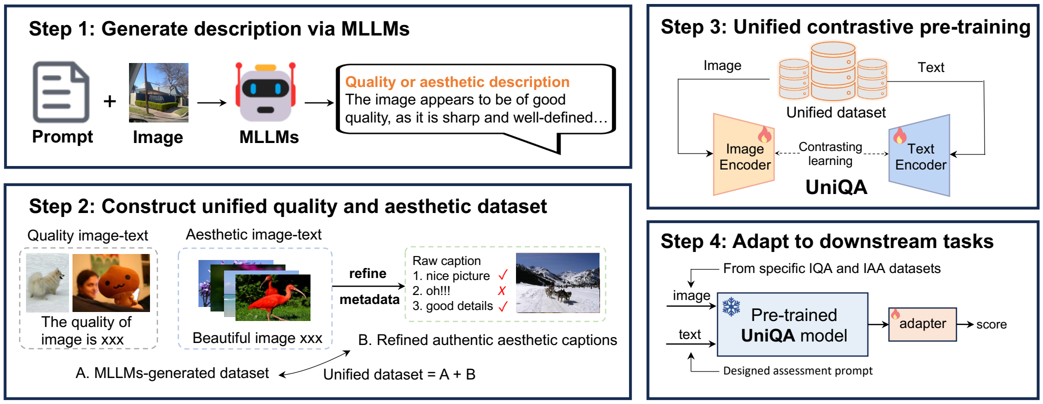

Figure 1: The overview of our method. We leverage MLLMs to generate quality- and aesthetics-related descriptions (Step 1) and utilize the generated data to refine authentic noisy data (Step 2). We conduct unified pre-training to obtain UniQA (Step 3), which can be flexibly applied to both IQA and IAA tasks with a lightweight adapter (Step 4).

(UniQA) to extract mutually beneficial and effective representations for both tasks. Then, the pre-trained UniQA can be flexibly applied to IQA and IAA datasets.

To achieve unified pre-training, a straightforward solution involves consolidating all IQA and IAA datasets and then training the model to regress towards the mean opinion scores (MOS) annotated by humans. However, existing datasets show variations in perceptual scales due to differences in subjective testing methodologies (Zhang et al., 2021a). As a result, this training strategy makes the model develop a score bias toward larger scale datasets. Moreover, it may not effectively capture the unique characteristics of IQA and IAA, as the MOS labels cannot be explicitly interpreted. To this end, we propose to use **text descriptions** as a bridge to integrate the two tasks, leveraging the rich and fine-grained semantics inherent in text to provide more auxiliary information.

However, existing IQA datasets typically have images only and lack text descriptions. While current IAA datasets (Ghosal et al., 2019) include text data provided by humans, they often contain considerable textual noise irrelevant for aesthetic assessment. Therefore, a top priority is determining how to acquire high-quality image-text data for both IQA and IAA tasks. Recently, multimodal large language models (MLLMs) (Liu et al., 2023b; Zhu et al., 2023; Lin et al., 2023; Bai et al., 2023) have demonstrated outstanding capabilities in image understanding, which can generate reasonable responses based on images and user instructions. Inspired by this, we propose utilizing MLLMs with tailored prompts to generate quality- and aesthetics-related descriptions for the IQA and IAA datasets, respectively (Step 1 of Figure 1). As observed in Figure 2, this approach provides a comprehensive and precise depiction of image quality and aesthetics. Furthermore, we utilize these generated high-quality aesthetics-related descriptions as metadata to refine the raw aesthetic caption dataset (Step 2 of Figure 1). Finally, we unify the generated and refined image-text datasets to conduct vision-language contrast pre-training (Step 3 of Figure 1). This results in the pre-trained UniQA with a powerful multimodal image assessment perception.

After pre-training on image-text pairs, we propose a lightweight adapter, namely the Multi-Cue Integration Adapter, to fine-tune the specific dataset of two tasks (Step 4 of Figure 1). This adapter uses versatile cues related to image assessment to prompt the pre-trained UniQA, adeptly extracting useful knowledge and comprehensively assessing the image. With much fewer tunable parameters compared to previous IQA and IAA models, our model outperforms them on both tasks. More surprisingly, benefiting from the powerful representations learned by pre-training, our method achieves impressive results on few-label IQA, *e.g.*, achieving the SRCC values of 0.828 (vs. 0.760 on CLIVE of GRepQ (Srinath et al., 2024)) and 0.844 (vs. 0.812 on KonIQ of GRepQ).

Our contributions can be summarized as follows:

- With the assistance of MLLMs, we construct a high-quality image-text dataset about image quality and aesthetics. Through pre-training on this dataset, we develop UniQA, which effectively learns a general perception of image assessment, promoting the effective and efficient learning of both IQA and IAA tasks.

- We propose a novel Multi-Cue Integration Adapter, which integrates various assessment-related cues to fully exploit the extensive knowledge of the pre-trained model with minimal additional parameters.
- Extensive experiments show that our method achieves SOTA performance across multiple IQA and IAA datasets. Benefiting from the rich representations learned through pre-training, UniQA also demonstrates exceptional few-label image assessment capabilities.

2 Related Work

Image Quality Assessment. The rapid development of deep learning has sparked significant interest in their application for IQA. Many researchers utilize CNN to solve the IQA problem with various effective techniques, including multi-level feature aggregation (Li et al., 2018), adaptive quality prediction (Su et al., 2020), and patch-to-picture learning (Ying et al., 2020), order learning (Shin et al., 2024) and unsupervised learning (Saha et al., 2023). Recently, transformer-based IQA methods (Ke et al., 2021; Zhu et al., 2021; Qin et al., 2023; Xu et al., 2024; Yu et al., 2024) show promising results in the IQA field, which can compensate for the non-local representation ability of CNN. Despite these impressive breakthroughs, these methods often transfer models pre-trained on classification datasets, such as ImageNet (Deng et al., 2009), to IQA tasks, which may be suboptimal (Li et al., 2023d). Q-Align (Wu et al., 2023b) attempts to jointly perform IQA and IAA tasks, but it uses a language model with a huge number of parameters and does not explicitly extract features of the two tasks through pre-training. Our method can learn more effective representations through joint pre-training on quality-aesthetics image-text data, providing benefits for IQA tasks.

Image Aesthetic Assessment. With the advent of deep learning, IAA methods have evolved from hand-crafted feature extraction (Datta et al., 2006; Ke et al., 2006; Nishiyama et al., 2011; Sun et al., 2009) to end-to-end feature learning, marking significant advancements in the IAA domain. Various techniques have been developed to boost IAA task, including local and global feature integration (Lu et al., 2015; Hou et al., 2020; Shi et al., 2024; Huang et al., 2024a; He et al., 2023b), graph network (She et al., 2021; Duan et al., 2022) and theme-aware learning (Li et al., 2023c; He et al., 2022). Recently, there has been an emergence of multimodal IAA methods (Zhang et al., 2020; Zhou et al., 2016; Zhang et al., 2021b; Nie et al., 2023; Huang et al., 2024b) that incorporate text as auxiliary supervision. However, these methods necessitate the use of text during inference, limiting their flexible application since text is often not easily available. Our method overcomes this limitation by conducting vision-language pre-training firstly to learn effective representation. The pre-trained model can be flexibly applied to the IAA field using only images.

Vision-Language Models. Vision-Language Models (VLMs) (Radford et al., 2021; Jia et al., 2021; Yao et al., 2021; Yu et al., 2022; Sun et al., 2023) introduce the contrastive learning strategy to acquire image-text correspondences from large-scale image-text pairs. VLMs have exhibited promising results across multiple tasks, including IQA (Wang et al., 2023; Zhang et al., 2023b) and IAA (Hentschel et al., 2022; Sheng et al., 2023). Recently, the Multimodal Large Language Models (MLLMs) have garnered increasing research interest, exhibiting remarkable prowess in comprehending image content and reasoning through complex instructions (Liu et al., 2023b; Zhu et al., 2023; Li et al., 2023a; Ye et al., 2023; Bai et al., 2023). Most existing MLLMs achieve this by integrating image features with LLM tokens, subsequently fine-tuning the LLM via multimodal instruction tuning. During inference, MLLMs can reason with given images and user instructions, generating text responses by leveraging world knowledge learned during pre-training.

3 UniQA: MLLMs-assisted Unified Pre-training

In this section, we first present some preliminaries of related models (Section 3.1). We then describe the process of constructing a unified image-text dataset about quality and aesthetics, with the assistance of MLLMs (Section 3.2 and 3.3). We use this dataset to pre-train the vision-language model (Section 3.4) to construct our UniQA.

Quality-related captioning
MOS of image: 7.36 → **Text level**: good
Prompt: What you are given is a good quality image. Evaluate image quality based on factors such as *sharpness, color balance, and noise level*.
Output: The image is of a living room with a fireplace, a couch, a chair, and a coffee table. The room is well-lit, and the fireplace adds warmth to the space. The image is of high quality, with good resolution, minimal noise, and appropriate brightness levels.

Aesthetics-related captioning
MOS of image: 4.86 → **Text level**: fair
Prompt: What you get is an image of fair aesthetics. Evaluate image aesthetics based on factors such as *content, color, lighting, and composition*.
Output: The image presents a medium aesthetic quality, with a focus on the snow-covered highway and the mountain range in the background. The overall composition of the image is balanced, with highways and mountains as the main subjects, and the cars and trees providing additional interest and context.

Figure 2: Generated quality- and aesthetics-related captions via MLLMs. The red text refers to MOS-based text guidance. The orange text highlights the quality- and aesthetics-related text.

3.1 Preliminaries

Vision-language pre-training aims to achieve comprehensive cross-modality understanding by training on web-scale image-text datasets. Benefiting from this large-scale pre-training, CLIP (Radford et al., 2021), a prominent VLM, has demonstrated great promise to assist a broad scope of vision tasks. Specifically, CLIP comprises an image encoder f and a text encoder g, both jointly trained to establish a shared latent space for image and text through contrastive learning.

Given a batch of N paired images and texts $\{x_I^i, x_T^i\}_{i=1}^N$, CLIP extracts image features $\boldsymbol{I} = \{f(x_I^i)\}_{i=1}^N$ and text features $\boldsymbol{T} = \{g(x_T^i)\}_{i=1}^N$ with corresponding encoders. During pre-training, CLIP seeks to maximize the cosine similarity of paired image and text features, while minimizing the similarity of unmatched pairs. The contrastive learning objective can be formulated as:

$$\begin{aligned} \mathcal{L}_{\text{image}} &= -\mathbb{E}_{I_i \sim \boldsymbol{I}} \left[\log \frac{\exp(I_i^\top T_i / \tau)}{\sum_{j=1}^N \exp(I_i^\top T_j / \tau)} \right] \\ \mathcal{L}_{\text{text}} &= -\mathbb{E}_{T_i \sim \boldsymbol{T}} \left[\log \frac{\exp(T_i^\top I_i / \tau)}{\sum_{j=1}^N \exp(T_i^\top I_j / \tau)} \right] \end{aligned} \tag{1}$$

where the I_i and T_i are the i-th features in the batch, and τ is the temperature parameter. The final contrastive learning loss can be obtained by taking the average: $\mathcal{L} = (\mathcal{L}_{\text{image}} + \mathcal{L}_{\text{text}})/2$. With this training strategy, CLIP can generate aligned features in latent space for paired image-text samples.

3.2 Quality- and Aesthetics-related Captioning

In order to achieve vision-language pre-training in the field of image assessment, we need to generate text for IQA and IAA datasets since IQA datasets lack text and IAA datasets contain noisy text. Recently, MLLMs have shown advanced performance, so we can use them to generate high-quality textual data for images. Previous studies (Wu et al., 2023a; Huang et al., 2024c) have highlighted that it is challenging for MLLMs to directly and accurately perceive the quality and aesthetics of input images, often resulting in positively skewed expressions and strong hallucinations (see examples in Appendix D). Thus, to obtain correct and detailed descriptions about quality and aesthetics, as shown in Figure 2, we design ***MOS-guided task-specific prompts*** to instruct MLLMs:

$$Y_t \sim M_T(x_I, P_t | G). \tag{2}$$

where M_T denotes the used MLLM, G is the MOS-based text guidance, P_t is the task-specific prompt, Y_t represents the generate caption. To obtain G, we divide images into 5 levels based on MOS, *i.e.*, $\{$`bad`, `poor`, `fair`, `good`, `perfect`$\}$ (Ghadiyaram & Bovik, 2015; Sheikh et al., 2006; Zhang et al., 2023b). If an image's MOS ranks in the top 20% of the score range, its level is assigned to `perfect`. This approach harmonizes IQA and IAA datasets with different MOS scales, alleviating the MOS biases of different datasets (Zhang et al., 2021a). Additionally, P_t is customized for IQA (P_{IQA}) and IAA (P_{IAA}) tasks, respectively. As shown in Figure 2, P_{IQA} involves *sharpness, color balance, and noise level* (Chandler, 2013), while P_{IAA} includes *content, color, lighting, and composition* (Deng et al., 2017). With these designs, M_T is guided towards image assessment

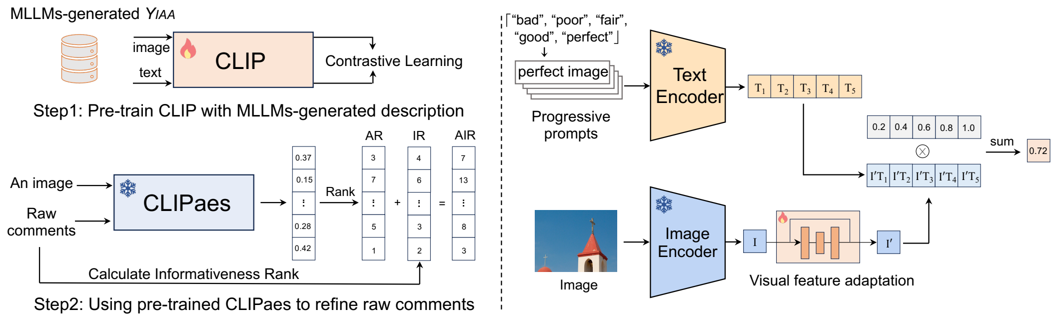

(a) Data purification process

(b) Multi-Cue Integration Adapter

Figure 3: (a) Data purification process: we pre-train CLIP using generated aesthetic captions data Y_{IAA} and then use the pre-trained CLIP_{aes} to purify data. (b) The proposed adapter: we employ progressive prompts, {`bad`, `poor`, `fair`, `good`, `perfect`} with "image", to prompt the frozen UniQA and a lightweight trainable module to adjust visual features.

and we can obtain generated caption datasets Y_{IQA} and Y_{IAA} for IQA and IAA tasks, respectively. For simplicity and cost-effectiveness, we use open-source LLaVa (Liu et al., 2023a) as the captioner. We also experiment with the effects of different MLLMs on model performance (Table 6).

3.3 Data Purification Strategy

In addition to the generated aesthetic captions Y_{IAA}, there are also IAA datasets with captions commented by humans (Ghosal et al., 2019), which directly reflect human aesthetic feelings. Incorporating comments from various people can offer a more comprehensive description of image aesthetics. However, while enhancing text diversity, it may introduce noise to the data, as individuals may provide comments unrelated to image aesthetics. To address this issue, we propose a novel data purification strategy to refine raw captions in the original dataset. This process is illustrated in Figure 3(a).

Specifically, we introduce ***Aesthetics-relevance and Informativeness Rank (AIR)*** to measure the quality of text corresponding to an image. The AIR consists of Aesthetics-relevance Rank (AR) and Informativeness Rank (IR). To obtain AR, we first pre-train a CLIP model with generated aesthetic data Y_{IAA} to get an aesthetics-aware CLIP model, denoted as CLIP_{aes}. Then, we employ it to measure the aesthetics relevance score (s_A) for an image-text pair. Given an image with n captions, AR can be defined as:

$$\text{AR} = \text{Rank}(s_A^1 \cdots s_A^n), \quad s_A^i = \text{CLIP}_{\text{aes}}(x_I, x_T^i), \tag{3}$$

where s_A^i represents the aesthetics relevance score between the i-th caption x_T^i and its corresponding image x_I. Note that AR consists of *long integers* that represent the rank of a caption after sorting by s_A. To obtain IR, we simply utilize the sentence length as informativeness score (s_I) to measure the informativeness of text. Accordingly, for an image with n textual captions, IR can be expressed as:

$$\text{IR} = \text{Rank}(s_I^1, \cdots, s_I^n), \quad s_I^i = \text{Length}(x_T^i), \tag{4}$$

where $\text{Length}(\cdot)$ is able to output the length of an input sentence. As a result, AIR between an image and n captions is:

$$\text{AIR} = \text{Rank}((\text{AR}^1 + \text{IR}^1), \cdots, (\text{AR}^n + \text{IR}^n)). \tag{5}$$

We select captions with Top-K ranking AIR to construct a high-quality aesthetic caption dataset, denoted as Y_{IAA}^+. This strategy ensures the preservation of text that is both related to aesthetic perception and rich in information, thereby enhancing the quality and richness of the raw dataset.

3.4 Unified Vision-Language Pre-training

So far, we have gotten a high-quality image-text dataset about quality and aesthetics, $Y = Y_{IQA} \cup Y_{IAA} \cup Y_{IAA}^+$. Based on it, we pre-train CLIP using Equation 1 to obtain our UniQA. In this way, the model learns general perceptions of image quality and aesthetics, which can provide potent assessment priors and thus can be effectively applied to both IQA and IAA tasks.

4 Adapting Vision-Language Model for IQA and IAA

The pre-trained UniQA contains extensive perception information, which can facilitate downstream assessment tasks in a zero-shot or supervised manner. In this section, we further propose a meticulously designed adapter (Section 4.1) and prompt ensemble strategy (Section 4.2) to enhance the model's performance.

4.1 Multi-Cue Integration Adapter

During pre-training, the model aligns image and assessment-related captions, empowering it with strong comprehension of image quality and aesthetics. With this foundation model, we can slightly adjust the visual features, efficiently adapting it to score-based image assessment tasks. To this end, we introduce a lightweight adapter, namely the ***Multi-Cue Integration Adapter***, to adapt visual features and inject rich cues for fine-tuning downstream tasks. The adapter consists of two key processes: visual feature adaptation and multi-cue integration prediction.

Visual Feature Adaptation. We add a learnable residual module following the pre-trained image encoder to adjust the visual features so as to adapt to specific assessment datasets. We optimize this module while keeping the image and text backbones frozen, enabling parameter-efficient tuning. The structure of the adapter is illustrated in Figure 3(b). Let I denote the image features extracted from the frozen image encoder, the visual feature adaptation process can be expressed as:

$$I' = \mathrm{Normalize}(\mathrm{Adapter}(I) + I) \tag{6}$$

where the $\mathrm{Adapter}(\cdot)$ consists of two fully connected layers with a ReLU activation in between, and I' represents the adapted visual features.

Multi-cue Integration Prediction. A straightforward approach to incorporating the CLIP model into perception assessment is to utilize the "`good image`" as an anchor and take the cosine similarity between the text anchor and a given image as the assessment score. However, this method shows two shortcomings: (1) using the absolute value of similarity as the perception score may not be optimal because it only reflects the semantic similarity between images and texts (Wu et al., 2023a; Wang et al., 2023); (2) a single prompt may not fully leverage the extensive knowledge of the pre-trained model. Thus, we propose to utilize versatile cues to comprehensively explore the power of the pre-trained UniQA and convert absolute similarity scores into relative values for weighting.

Specifically, we utilize the prompt template "{level} image" and five text levels (`bad`, `poor`, `fair`, `good`, `perfect`), *i.e.*, "*Multi-cue*", to construct prompts. Next, we calculate the cosine similarity between the normalized text features $\{T_i\}_{i=1}^5$ of five prompts and adapted visual features I', and then use the $\mathrm{Softmax}(\cdot)$ to obtain the related value of five image-text correspondence. These related values will weight the predefined score levels to get the final assessment score. This process can be formulated as follows:

$$q = \sum_{i=1}^{5} \frac{c_i \exp(I'^\top T_i/\tau)}{\sum_{j=1}^{5} \exp(I'^\top T_i/\tau)}, \tag{7}$$

where $\{c_i\}_{i=1}^5$ are scores of text levels with progressive values that are set to $\{0.2, 0.4, 0.6, 0.8, 1.0\}$; τ is the temperature parameter and q is the assessment score of the given image.

4.2 Prompt Ensemble Strategy

We introduce the prompt ensemble strategy, which incorporates more prompt groups to derive the final assessment score, thereby achieving a more comprehensive understanding of image quality and aesthetics. For instance, we can use *e.g.*, {`extremely blurry`, `blurry`, `fair`, `sharp`, `extremely sharp`} as another five text levels. Now, the final assessment score q_f is the average of all prompt groups and it can be described as:

$$q_f = \frac{\sum_{i=1}^{m} q_i}{m}, \tag{8}$$

where m denotes the number of prompt groups. This strategy can more fully utilize the multi-modal understanding capabilities of the pre-trained UniQA and demonstrates non-negligible performance improvements in zero-shot (Table 4) and few-label supervised learning (Table 5). The details of ensemble prompts are attached in supplementary material.

Table 1: Results on IQA datasets. **Black** and **blue** numbers in bold represent the best and second best, respectively. Higher SRCC and PLCC imply better performance.

	TID2013		CSIQ		KADID		CLIVE		KonIQ		SPAQ	
Method	SRCC	PLCC	SRCC	PLCC	SRCC	PLCC	SRCC	PLCC	SRCC	PLCC	SRCC	PLCC
WaDIQaM (Bosse et al., 2017)	0.835	0.855	0.852	0.844	0.739	0.752	0.682	0.671	0.804	0.807	0.840	0.845
DBCNN (Zhang et al., 2018)	0.816	0.865	0.946	0.959	0.851	0.856	0.851	0.869	0.875	0.884	0.911	0.915
MetaIQA (Zhu et al., 2020)	0.856	0.868	0.899	0.908	0.762	0.775	0.802	0.835	0.850	0.887	-	-
PaQ-2-PiQ (Ying et al., 2020)	0.862	0.856	0.899	0.902	0.840	0.849	0.844	0.842	0.872	0.885	-	-
HyperIQA (Su et al., 2020)	0.840	0.858	0.923	0.942	0.852	0.845	0.859	0.882	0.906	0.917	0.911	0.915
TReS (Golestaneh et al., 2022)	0.863	0.883	0.922	0.942	0.859	0.858	0.846	0.877	0.915	0.928	-	-
MUSIQ (Ke et al., 2021)	0.773	0.815	0.871	0.893	0.875	0.872	0.702	0.746	0.916	0.928	0.918	0.921
DACNN (Pan et al., 2022)	0.871	0.889	0.943	0.957	0.905	0.905	0.866	0.884	0.901	0.912	0.915	0.921
DEIQT (Qin et al., 2023)	**0.892**	**0.908**	0.946	**0.963**	0.889	0.887	0.875	0.894	0.921	0.934	0.919	0.923
LIQE (Zhang et al., 2023b)	-		0.936	0.939	0.930	0.931	**0.904**	**0.911**	0.919	0.908	-	-
Re-IQA (Saha et al., 2023)	0.804	0.861	**0.947**	0.960	0.872	0.885	0.840	0.854	0.914	0.923	0.918	0.925
LoDA (Xu et al., 2024)	0.869	0.901	-	-	**0.931**	**0.936**	0.876	0.899	0.932	**0.944**	**0.925**	**0.928**
Q-Align (Wu et al., 2023b)	-	-	0.915	0.936	0.869	0.927	**0.931**	**0.921**	**0.935**	0.934	-	-
Ours	**0.916**	**0.931**	**0.963**	**0.973**	**0.940**	**0.943**	0.890	0.905	**0.933**	**0.941**	**0.924**	**0.928**

Table 2: Results on AVA.

Method	SRCC	PLCC
NIMA	0.612	0.636
MaxViT	0.708	0.745
APM	0.709	-
MUSIQ	0.726	0.738
MLSP	0.756	0.757
TANet	0.758	0.765
MILNet	0.732	0.753
EAT	0.759	0.77
VILA	**0.774**	**0.774**
Ours	**0.776**	**0.776**

Table 3: Results on AADB dataset.

Method	SRCC	PLCC
NIMA	0.708	0.711
MLSP	0.725	0.726
MUSIQ	0.706	0.712
PA-IAA	0.720	0.728
HIAA	0.739	-
TANet	0.738	0.737
Celona *et al.*	0.757	0.762
TAVAR	**0.761**	**0.763**
Ours	**0.786**	**0.787**

Table 4: SRCC on the zero-shot setting. * denotes using ensemble prompts. The results of other methods are pre-trained on FLIVE.

Method	CLIVE	KonIQ	AGIQA-3K
DBCNN	0.724	0.716	0.645
PaQ-2-PiQ	0.738	0.755	0.502
HyperIQA	0.735	0.758	0.629
TReS	0.740	0.713	0.646
DEIQT	**0.781**	**0.733**	-
CLIP*	0.746	0.592	0.646
Ours	0.638	0.667	**0.744**
Ours*	**0.790**	**0.806**	**0.752**

5 EXPERIMENTS

5.1 DATASETS

We employ the IQA dataset FLIVE (Ying et al., 2020) and the IAA dataset AVA (Murray et al., 2012) for quality- and aesthetics-related captioning, respectively, and AVA-Captions (Ghosal et al., 2019) to provide authentic aesthetic comments. We evaluate the performance on typical IQA and IAA datasets, including seven IQA datasets and two IAA datasets.

IQA Dataset. For the IQA task, four synthetic datasets, including LIVE (Sheikh et al., 2006), CSIQ (Larson & Chandler, 2010), TID2013 (Ponomarenko et al., 2013), KADID (Lin et al., 2019), and three authentic datasets of CLIVE (Ghadiyaram & Bovik, 2015), KonIQ (Hosu et al., 2020), SPAQ (Fang et al., 2020), are used for performance evaluation. FLIVE (Ying et al., 2020) is an authentic IQA dataset that contains 39,810 images. We employ an AIGC-generated IQA dataset, AGIQA-3K (Li et al., 2023b), to evaluate the generalization capability of our UniQA. Details of the datasets can be found in appendix.

IAA Dataset. For the IAA task, we conduct experiments on AVA (Murray et al., 2012) and AADB (Kong et al., 2016) datasets. AVA comprises 250k images, with the test set of 19,928 images. AADB dataset consists of 10,000 images in total, with 8,500 images for training, 500 images for validation, and 1,000 images for testing.

AVA-Captions Dataset. AVA-Captions (Ghosal et al., 2019) offer multiple human-annotated comments for each AVA image. To avoid potential data leakage, we strictly follow the official data split of AVA, results in a pre-training image-text dataset comprising 234,090 images paired with 3.0 million captions.

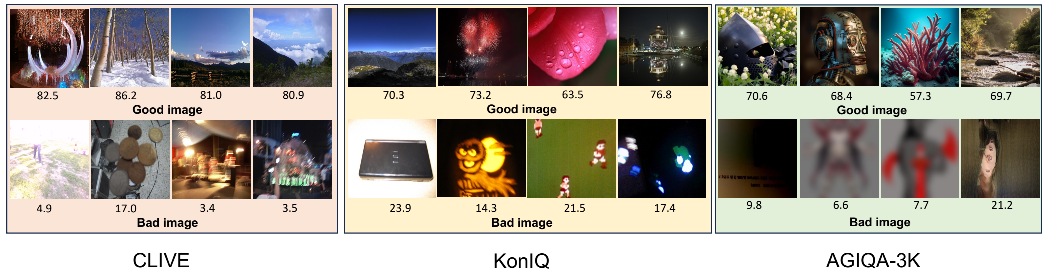

Figure 4: The image retrieval results on three dataset with varied prompts. The number below the image is its MOS label. Zoom in for a better view.

Table 5: SRCC results using few labels for training. * denotes using ensemble prompts.

	CLIVE			KonIQ			LIVE		
Method	50	100	200	50	100	200	50	100	200
HyperIQA (Su et al., 2020)	0.648	0.725	0.790	0.615	0.710	0.776	0.892	0.912	0.929
TReS (Golestaneh et al., 2022)	0.670	0.751	0.799	0.713	0.719	0.791	0.901	0.927	**0.957**
ResNet50 (He et al., 2016)	0.576	0.611	0.636	0.635	0.670	0.707	0.871	0.906	0.922
CLIP (Radford et al., 2021)	0.664	0.721	0.733	0.736	0.770	0.782	0.896	0.923	0.941
CONTRIQUE (Madhusudana et al., 2022)	0.695	0.729	0.761	0.733	0.794	0.821	0.891	0.922	0.943
CLIPIQA (Wang et al., 2023)	0.646	0.611	0.642	0.579	0.620	0.667	0.633	0.724	0.784
Re-IQA (Saha et al., 2023)	0.591	0.621	0.701	0.685	0.723	0.754	0.884	0.894	0.929
DEIQT (Qin et al., 2023)	0.667	0.718	0.812	0.638	0.682	0.754	0.920	**0.942**	0.955
GRepQ (Srinath et al., 2024)	**0.760**	**0.791**	**0.822**	**0.812**	**0.832**	**0.855**	**0.926**	0.937	0.953
Ours	0.813	0.836	0.850	0.772	0.842	0.870	0.962	0.956	0.974
Ours*	**0.828**	**0.849**	**0.853**	**0.844**	**0.860**	**0.876**	**0.963**	**0.958**	**0.976**

5.2 Implementation Details

We use CLIP-B/16 (Radford et al., 2021) as our VLM for pre-training and LLaVA-1.5-7B (Liu et al., 2023b;a) as our MLLM for captioning. We pre-train the model using Adam optimizer (Kingma & Ba, 2014) with a learning rate of 5e-6 and weight decay of 0.2. The model is trained for 5 epochs with a batch size of 960. We set $K = 4$ to refine the AVA-Captions dataset. We use MSE loss to optimize the adapter on downstream tasks and different training settings according to the task and size of datasets. More training details are provided in the appendix. For each IQA dataset, 80% of the images are used for training and the remaining 20% for testing. We repeat this process 10 times to mitigate the performance bias and the medians of SRCC and PLCC are reported. For the IAA datasets, we follow the standard data splits.

5.3 Main Results

Results on IQA task. Table 1 reports the performance of the SOTA IQA methods on six typical IQA datasets. The results of LIVE (Sheikh et al., 2006) are presented in the supplementary material due to page limitations. Our method demonstrates a substantial superiority over existing SOTA models across a diverse range of datasets, fully confirming the effectiveness and excellence of our method in precisely characterizing image quality.

Results on IAA task. We report the experimental results on the AVA (Murray et al., 2012) and AADB (Kong et al., 2016) datasets in Table 2 and Table 3, respectively. Given that the pre-trained model acquired a unified and robust image assessment perception, it can also achieve SOTA results after fine-tuning on these two datasets. These results validate that our method can be effectively applied to both IQA and IAA domains.

5.4 Generalization Capability Validation

Table 4 evaluate the generalization capability of our model. Unlike previous methods that train on one dataset and test on others, we directly utilize the pre-trained UniQA and textual prompts for image quality assessment. This presents a more challenging setting as the model isn't optimized on MOS labels. As observed, our method achieves the best performance on these three datasets. Notably, our method demonstrates excellent performance on AIGC-generated images AGIQA-3K (Li

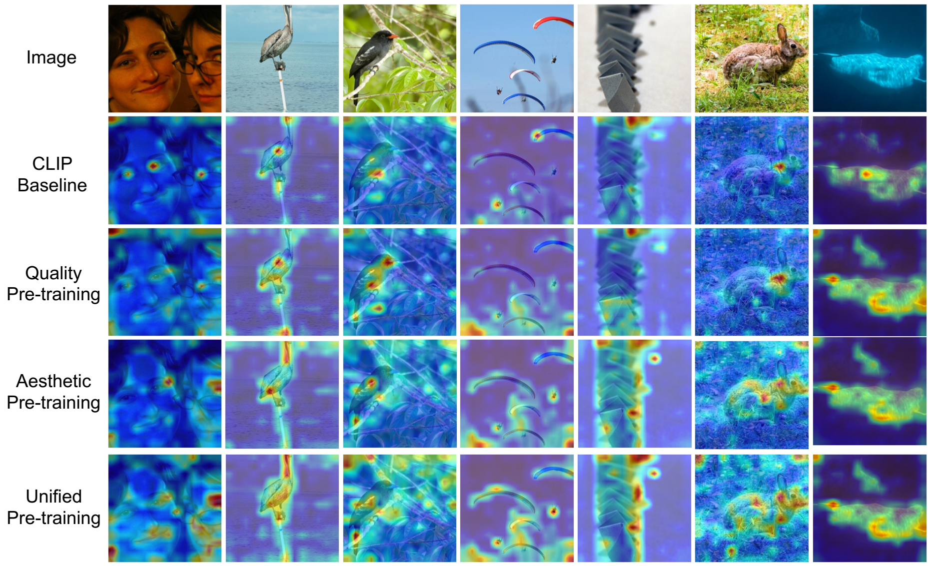

Figure 5: Grad-CAM (Selvaraju et al., 2017) visualization of different pre-training for prompt “blurry image”. Through pre-training, the model focuses more on noisy objects and backgrounds.

et al., 2023b), which are markedly different from images of natural scenes. These results demonstrate the strong generalization capability of our UniQA. Additionally, the UniQA outperforms the original CLIP significantly, proving the effectiveness of our quality- and aesthetics-related pre-training.

We use different text queries to calculate the image-text similarity and rank them to achieve zero-shot image retrieval. Figure 4 demonstrates the visualization of the top retrieval results. We notice that the retrieved results of “good image” exhibit sharp and aesthetically pleasing images, whereas “bad image” prompts retrieve blurry, poor lighting and meaningless images. These examples provide qualitative evidence of the quality and aesthetic knowledge captured by the pre-trained model.

Table 6: Ablation on IQA (CLIVE and KonIQ) and IAA (AVA) datasets with SRCC metrics.

Ablation type	CLIVE	KonIQ	AVA
Ablation on different pre-training data			
Y_{IQA} Y_{IAA} Y^{+}_{IAA}			
× × ×	0.865	0.907	0.748
✓ × ×	0.871	0.914	0.755
× ✓ ×	0.871	0.917	0.755
✓ ✓ ×	0.874	0.918	0.756
× × ✓	0.875	0.928	0.773
× ✓ ✓	0.877	0.930	0.774
✓ ✓ ✓	**0.890**	**0.933**	**0.776**
Ablation on data purification strategy			
w/o Strategy	0.876	0.929	0.772
IR Strategy	0.879	0.931	0.774
AR Strategy	0.885	0.930	0.774
AIR Strategy	**0.890**	**0.933**	**0.776**
Ablation on the proposed adapter			
Single Prompt	0.705	0.920	0.765
Antonym Prompt	0.875	0.928	0.771
Ours adapter	**0.890**	**0.933**	**0.776**
Ablation on different MLLMs			
LLaVA-v1.5-7B	0.871	0.914	0.755
LLaVA-v1.5-13B	0.872	0.914	0.757
Sphinx	0.874	0.916	0.758
QWen-VL	0.870	0.913	0.757
LLaVa-7B+QWen	0.875	0.916	0.758
Sphinx+QWen	**0.877**	**0.918**	**0.759**

5.5 Data-Efficient Learning

The pre-trained model acquires extensive image assessment knowledge, providing robust priors for downstream tasks. Consequently, our model can deliver impressive performance with limited data. To validate this, we randomly select subsets of 50, 100, and 200 samples from the training set for training and evaluate them on the same test data as full-data supervised learning. We report the median performance across 10 times in Table 5. Our method notably outperforms the second-best model GRepQ by a substantial margin, even though GRepQ is specifically designed for data-efficient learning. These results thoroughly demonstrate the potent capability of our method to learn image quality even when only a few labels are available. Additionally, several insightful observations can be drawn from Table 5. Firstly, the prompt ensemble strategy markedly enhances model performance in the data-efficient setting. This is attributed to its ability to more fully leverage the extensive knowledge of the pre-trained model. Secondly, the impact of prompt ensemble is slight on synthetic datasets. This is likely due to the limited image variety within synthetic datasets, making a single prompt sufficient for such scenarios.

5.6 Ablation Studies

Impact of different pre-training data. Table 6 shows the effect of different pre-training data. We observe that unified pre-training achieves the optimal performance on both tasks. In addition, we derive some meaningful observations. (1) Using either the generated Y_{IQA} or Y_{IAA} improves the performance of both IQA and IAA tasks, proving the mutual benefit of these two tasks and the effectiveness of MLLMs captioning. (2) Unifying Y_{IQA} and Y_{IAA} datasets does not lead to significant improvements. We believe this is because the MLLMs-generated text tends to have similar sentence structures (Liu et al., 2023c) and perception representation, limiting the diversity provided for multimodal learning. (3) Pre-training with refined authentic Y_{IAA}^{+} shows significant improvement on two tasks, reflecting that human-annotated comments can provide a more comprehensive and effective representation for the model.

Figure 5 illustrates the Grad-CAM (Selvaraju et al., 2017) visualization of different pre-training. We can notice that after quality-related and aesthetic pre-training, the model pays more attention to blurred subjects and noisy backgrounds. This effect becomes more pronounced with unified pre-training, underscoring the advantages of such a unified approach. In addition, the unified pre-training can focus on the areas of quality-related and aesthetic pre-training at the same time. This shows that unified training can learn common representations of the two tasks.

Effectiveness of data purification strategy. The second part of Table 6 illustrates the ablation study of the data purification strategy. It can be observed that employing either AR or IR strategy to purify data can improve the model's performance of both IQA and IAA tasks. These results validate the benefit of obtaining aesthetically relevant and semantically rich textual descriptions for the model. Finally, when combining these two strategies, it achieves the best performance.

Effectiveness of the Multi-Cue Integration Adapter. The third part of Table 6 shows the ablation study of the proposed adapter. "Single Prompt" denotes using the similarity between the text "good image" and images as the assessment score directly, while "Antonym Prompt" represents using the relative weights of texts "good image" and "bad image" to weight the predefined score. It is evident that the "Single Prompt" is considerably inferior to the "Antonym Prompt", showing the limitations of using semantic similarity as score directly. Our method integrates more cues into the "Antonym Prompt" to comprehensively assess images, thereby achieving optimal performance.

Ablation on different MLLMs. The bottom part of Table 6 presents the ablation study of various MLLMs. We generate Y_{IQA} via different MLLMs for pre-training. It is evident that using different MLLMs exhibits similar performance, while ensembling different MLLMs can boost performance. This indicates that MLLMs are capable of generating accurate captions with our text-guided prompt, and enhancing caption diversity can further improve performance. Considering resource limitations, we use LLaVa-7B and will integrate more MLLMs in the future.

6 Conclusion and Discussion

This paper introduces UniQA, which leverages unified vision-language pre-training to address quality and aesthetic assessment problems concurrently. We construct a high-quality image-text dataset about quality and aesthetics with the assistance of MLLMs. Through large-scale pre-training on this dataset, UniQA learns shared and effective representations of IQA and IAA tasks, benefiting both tasks. Additionally, we propose a Multi-Cue Integration Adapter to effectively adapt the pre-trained UniQA to downstream assessment tasks. Our method achieves state-of-the-art performance on both IQA and IAA tasks, and demonstrates powerful zero-shot and few-label image assessment capabilities.

Limitations and future work. MLLMs often generate captions with similar sentence structures and semantic expressions, restricting their ability to provide diverse and enriched representations for multimodal learning. Future work will explore other techniques to address this issue, including integrating various MLLMs for captioning and employing in-context learning methods.

REFERENCES

Nasim Jamshidi Avanaki, Abhijay Ghildyal, Nabajeet Barman, and Saman Zadtootaghaj. Lar-iqa: A lightweight, accurate, and robust no-reference image quality assessment model. *arXiv preprint arXiv:2408.17057*, 2024.

Jinze Bai, Shuai Bai, Shusheng Yang, Shijie Wang, Sinan Tan, Peng Wang, Junyang Lin, Chang Zhou, and Jingren Zhou. Qwen-vl: A versatile vision-language model for understanding, localization, text reading, and beyond. 2023.

Sebastian Bosse, Dominique Maniry, Klaus-Robert Müller, Thomas Wiegand, and Wojciech Samek. Deep neural networks for no-reference and full-reference image quality assessment. *IEEE TIP*, 27(1):206–219, 2017.

Damon M Chandler. Seven challenges in image quality assessment: past, present, and future research. *International Scholarly Research Notices*, 2013, 2013.

Hangwei Chen, Xiongli Chai, Feng Shao, Xuejin Wang, Qiuping Jiang, Xiangchao Meng, and Yo-Sung Ho. Perceptual quality assessment of cartoon images. *IEEE Transactions on Multimedia*, 25:140–153, 2021.

Zijian Chen, Wei Sun, Haoning Wu, Zicheng Zhang, Jun Jia, Zhongpeng Ji, Fengyu Sun, Shangling Jui, Xiongkuo Min, Guangtao Zhai, et al. Exploring the naturalness of ai-generated images. *arXiv preprint arXiv:2312.05476*, 2023.

Ritendra Datta, Dhiraj Joshi, Jia Li, and James Z Wang. Studying aesthetics in photographic images using a computational approach. In *ECCV*, pp. 288–301. Springer, 2006.

Jia Deng, Wei Dong, Richard Socher, Li-Jia Li, Kai Li, and Li Fei-Fei. Imagenet: A large-scale hierarchical image database. In *CVPR*, pp. 248–255. Ieee, 2009.

Yubin Deng, Chen Change Loy, and Xiaoou Tang. Image aesthetic assessment: An experimental survey. *IEEE Signal Processing Magazine*, 34(4):80–106, 2017.

Jiachen Duan, Pengfei Chen, Leida Li, Jinjian Wu, and Guangming Shi. Semantic attribute guided image aesthetics assessment. In *2022 IEEE International Conference on Visual Communications and Image Processing (VCIP)*, pp. 1–5. IEEE, 2022.

Yuming Fang, Hanwei Zhu, Yan Zeng, Kede Ma, and Zhou Wang. Perceptual quality assessment of smartphone photography. In *CVPR*, pp. 3677–3686, 2020.

Honghao Fu, Yufei Wang, Wenhan Yang, and Bihan Wen. Dp-iqa: Utilizing diffusion prior for blind image quality assessment in the wild. *arXiv preprint arXiv:2405.19996*, 2024.

Deepti Ghadiyaram and Alan C Bovik. Massive online crowdsourced study of subjective and objective picture quality. *IEEE TIP*, 25(1):372–387, 2015.

Deepti Ghadiyaram and Alan C Bovik. Perceptual quality prediction on authentically distorted images using a bag of features approach. *Journal of vision*, 17(1):32–32, 2017.

Koustav Ghosal, Aakanksha Rana, and Aljosa Smolic. Aesthetic image captioning from weakly-labelled photographs. In *ICCV Workshops*, pp. 0–0, 2019.

S Alireza Golestaneh, Saba Dadsetan, and Kris M Kitani. No-reference image quality assessment via transformers, relative ranking, and self-consistency. In *WACV*, pp. 1220–1230, 2022.

Ke Gu, Dacheng Tao, Jun-Fei Qiao, and Weisi Lin. Learning a no-reference quality assessment model of enhanced images with big data. *IEEE transactions on neural networks and learning systems*, 29(4):1301–1313, 2017.

Kaiming He, Xiangyu Zhang, Shaoqing Ren, and Jian Sun. Deep residual learning for image recognition. In *CVPR*, pp. 770–778, 2016.

Shuai He, Yongchang Zhang, Rui Xie, Dongxiang Jiang, and Anlong Ming. Rethinking image aesthetics assessment: Models, datasets and benchmarks. In *IJCAI*, pp. 942–948, 2022.

Shuai He, Anlong Ming, Yaqi Li, Jinyuan Sun, ShunTian Zheng, and Huadong Ma. Thinking image color aesthetics assessment: Models, datasets and benchmarks. In *Proceedings of the IEEE/CVF International Conference on Computer Vision*, pp. 21838–21847, 2023a.

Shuai He, Anlong Ming, Shuntian Zheng, Haobin Zhong, and Huadong Ma. Eat: An enhancer for aesthetics-oriented transformers. In *ACM MM*, pp. 1023–1032, 2023b.

Simon Hentschel, Konstantin Kobs, and Andreas Hotho. Clip knows image aesthetics. *Frontiers in Artificial Intelligence*, 5:976235, 2022.

Vlad Hosu, Hanhe Lin, Tamas Sziranyi, and Dietmar Saupe. Koniq-10k: An ecologically valid database for deep learning of blind image quality assessment. *IEEE TIP*, 29:4041–4056, 2020.

Jingwen Hou, Sheng Yang, and Weisi Lin. Object-level attention for aesthetic rating distribution prediction. In *ACM MM*, pp. 816–824, 2020.

Yipo Huang, Leida Li, Pengfei Chen, Jinjian Wu, Yuzhe Yang, Yaqian Li, and Guangming Shi. Coarse-to-fine image aesthetics assessment with dynamic attribute selection. *IEEE Transactions on Multimedia*, 2024a.

Yipo Huang, Xiangfei Sheng, Zhichao Yang, Quan Yuan, Zhichao Duan, Pengfei Chen, Leida Li, Weisi Lin, and Guangming Shi. Aesexpert: Towards multi-modality foundation model for image aesthetics perception. In *Proceedings of the 32nd ACM International Conference on Multimedia*, pp. 5911–5920, 2024b.

Yipo Huang, Quan Yuan, Xiangfei Sheng, Zhichao Yang, Haoning Wu, Pengfei Chen, Yuzhe Yang, Leida Li, and Weisi Lin. Aesbench: An expert benchmark for multimodal large language models on image aesthetics perception. *arXiv preprint arXiv:2401.08276*, 2024c.

Chao Jia, Yinfei Yang, Ye Xia, Yi-Ting Chen, Zarana Parekh, Hieu Pham, Quoc Le, Yun-Hsuan Sung, Zhen Li, and Tom Duerig. Scaling up visual and vision-language representation learning with noisy text supervision. In *ICML*, pp. 4904–4916. PMLR, 2021.

Junjie Ke, Qifei Wang, Yilin Wang, Peyman Milanfar, and Feng Yang. Musiq: Multi-scale image quality transformer. In *ICCV*, pp. 5148–5157, 2021.

Yan Ke, Xiaoou Tang, and Feng Jing. The design of high-level features for photo quality assessment. In *CVPR*, volume 1, pp. 419–426. IEEE, 2006.

Jongyoo Kim and Sanghoon Lee. Fully deep blind image quality predictor. *IEEE Journal of selected topics in signal processing*, 11(1):206–220, 2016.

Diederik P Kingma and Jimmy Ba. Adam: A method for stochastic optimization. *arXiv preprint arXiv:1412.6980*, 2014.

Shu Kong, Xiaohui Shen, Zhe Lin, Radomir Mech, and Charless Fowlkes. Photo aesthetics ranking network with attributes and content adaptation. In *ECCV*, pp. 662–679. Springer, 2016.

Eric C Larson and Damon M Chandler. Most apparent distortion: full-reference image quality assessment and the role of strategy. *Journal of electronic imaging*, 19(1):011006–011006, 2010.

Bo Li, Yuanhan Zhang, Liangyu Chen, Jinghao Wang, Jingkang Yang, and Ziwei Liu. Otter: A multi-modal model with in-context instruction tuning. *arXiv preprint arXiv:2305.03726*, 2023a.

Chunyi Li, Zicheng Zhang, Haoning Wu, Wei Sun, Xiongkuo Min, Xiaohong Liu, Guangtao Zhai, and Weisi Lin. Agiqa-3k: An open database for ai-generated image quality assessment. *arXiv preprint arXiv:2306.04717*, 2023b.

Chunyi Li, Tengchuan Kou, Yixuan Gao, Yuqin Cao, Wei Sun, Zicheng Zhang, Yingjie Zhou, Zhichao Zhang, Weixia Zhang, Haoning Wu, et al. Aigiqa-20k: A large database for ai-generated image quality assessment. *arXiv preprint arXiv:2404.03407*, 2(3):5, 2024.

Dingquan Li, Tingting Jiang, Weisi Lin, and Ming Jiang. Which has better visual quality: The clear blue sky or a blurry animal? *IEEE TMM*, 21(5):1221–1234, 2018.

Leida Li, Hancheng Zhu, Sicheng Zhao, Guiguang Ding, and Weisi Lin. Personality-assisted multi-task learning for generic and personalized image aesthetics assessment. *IEEE TIP*, 29:3898–3910, 2020.

Leida Li, Yipo Huang, Jinjian Wu, Yuzhe Yang, Yaqian Li, Yandong Guo, and Guangming Shi. Theme-aware visual attribute reasoning for image aesthetics assessment. *IEEE TCSVT*, 2023c.

Xudong Li, Timin Gao, Xiawu Zheng, Runze Hu, Jingyuan Zheng, Yunhang Shen, Ke Li, Yutao Liu, Pingyang Dai, Yan Zhang, et al. Adaptive feature selection for no-reference image quality assessment using contrastive mitigating semantic noise sensitivity. *arXiv preprint arXiv:2312.06158*, 2023d.

Hanhe Lin, Vlad Hosu, and Dietmar Saupe. Kadid-10k: A large-scale artificially distorted iqa database. In *2019 Eleventh International Conference on Quality of Multimedia Experience (QoMEX)*, pp. 1–3. IEEE, 2019.

Ziyi Lin, Chris Liu, Renrui Zhang, Peng Gao, Longtian Qiu, Han Xiao, Han Qiu, Chen Lin, Wenqi Shao, Keqin Chen, et al. Sphinx: The joint mixing of weights, tasks, and visual embeddings for multi-modal large language models. *arXiv preprint arXiv:2311.07575*, 2023.

Haotian Liu, Chunyuan Li, Yuheng Li, and Yong Jae Lee. Improved baselines with visual instruction tuning. *arXiv preprint arXiv:2310.03744*, 2023a.

Haotian Liu, Chunyuan Li, Qingyang Wu, and Yong Jae Lee. Visual instruction tuning. *arXiv preprint arXiv:2304.08485*, 2023b.

Yanqing Liu, Kai Wang, Wenqi Shao, Ping Luo, Yu Qiao, Mike Zheng Shou, Kaipeng Zhang, and Yang You. Mllms-augmented visual-language representation learning. *arXiv preprint arXiv:2311.18765*, 2023c.

Xin Lu, Zhe Lin, Xiaohui Shen, Radomir Mech, and James Z Wang. Deep multi-patch aggregation network for image style, aesthetics, and quality estimation. In *ICCV*, pp. 990–998, 2015.

Kede Ma, Wentao Liu, Kai Zhang, Zhengfang Duanmu, Zhou Wang, and Wangmeng Zuo. End-to-end blind image quality assessment using deep neural networks. *IEEE Transactions on Image Processing*, 27(3):1202–1213, 2017.

Pavan C Madhusudana, Neil Birkbeck, Yilin Wang, Balu Adsumilli, and Alan C Bovik. Image quality assessment using contrastive learning. *IEEE TIP*, 31:4149–4161, 2022.

Xiongkuo Min, Ke Gu, Guangtao Zhai, Jing Liu, Xiaokang Yang, and Chang Wen Chen. Blind quality assessment based on pseudo-reference image. *IEEE Transactions on Multimedia*, 20(8): 2049–2062, 2017.

Anish Mittal, Anush Krishna Moorthy, and Alan Conrad Bovik. No-reference image quality assessment in the spatial domain. *IEEE Transactions on image processing*, 21(12):4695–4708, 2012a.

Anish Mittal, Rajiv Soundararajan, and Alan C Bovik. Making a “completely blind” image quality analyzer. *IEEE Signal processing letters*, 20(3):209–212, 2012b.

Naila Murray, Luca Marchesotti, and Florent Perronnin. Ava: A large-scale database for aesthetic visual analysis. In *CVPR*, pp. 2408–2415. IEEE, 2012.

Xixi Nie, Bo Hu, Xinbo Gao, Leida Li, Xiaodan Zhang, and Bin Xiao. Bmi-net: A brain-inspired multimodal interaction network for image aesthetic assessment. In *Proceedings of the 31st ACM International Conference on Multimedia*, pp. 5514–5522, 2023.

Masashi Nishiyama, Takahiro Okabe, Imari Sato, and Yoichi Sato. Aesthetic quality classification of photographs based on color harmony. In *CVPR*, pp. 33–40. IEEE, 2011.

Zhaoqing Pan, Hao Zhang, Jianjun Lei, Yuming Fang, Xiao Shao, Nam Ling, and Sam Kwong. Dacnn: Blind image quality assessment via a distortion-aware convolutional neural network. *IEEE TCSVT*, 32(11):7518–7531, 2022.

Nikolay Ponomarenko, Oleg Ieremeiev, Vladimir Lukin, Karen Egiazarian, Lina Jin, Jaakko Astola, Benoit Vozel, Kacem Chehdi, Marco Carli, Federica Battisti, et al. Color image database tid2013: Peculiarities and preliminary results. In *European workshop on visual information processing (EUVIP)*, pp. 106–111. IEEE, 2013.

Guanyi Qin, Runze Hu, Yutao Liu, Xiawu Zheng, Haotian Liu, Xiu Li, and Yan Zhang. Data-efficient image quality assessment with attention-panel decoder. *arXiv preprint arXiv:2304.04952*, 2023.

Alec Radford, Jong Wook Kim, Chris Hallacy, Aditya Ramesh, Gabriel Goh, Sandhini Agarwal, Girish Sastry, Amanda Askell, Pamela Mishkin, Jack Clark, et al. Learning transferable visual models from natural language supervision. In *ICML*, pp. 8748–8763. PMLR, 2021.

Avinab Saha, Sandeep Mishra, and Alan C Bovik. Re-iqa: Unsupervised learning for image quality assessment in the wild. In *CVPR*, pp. 5846–5855, 2023.

Ramprasaath R Selvaraju, Michael Cogswell, Abhishek Das, Ramakrishna Vedantam, Devi Parikh, and Dhruv Batra. Grad-cam: Visual explanations from deep networks via gradient-based localization. In *ICCV*, pp. 618–626, 2017.

Dongyu She, Yu-Kun Lai, Gaoxiong Yi, and Kun Xu. Hierarchical layout-aware graph convolutional network for unified aesthetics assessment. In *CVPR*, pp. 8475–8484, 2021.

Hamid R Sheikh, Muhammad F Sabir, and Alan C Bovik. A statistical evaluation of recent full reference image quality assessment algorithms. *IEEE TIP*, 15(11):3440–3451, 2006.

Xiangfei Sheng, Leida Li, Pengfei Chen, Jinjian Wu, Weisheng Dong, Yuzhe Yang, Liwu Xu, Yaqian Li, and Guangming Shi. Aesclip: Multi-attribute contrastive learning for image aesthetics assessment. In *ACM MM*, pp. 1117–1126, 2023.

Tengfei Shi, Chenglizhao Chen, Zhenyu Wu, Aimin Hao, and Yuming Fang. Improving image aesthetic assessment via multiple image joint learning. *ACM Transactions on Multimedia Computing, Communications and Applications*, 2024.

Nyeong-Ho Shin, Seon-Ho Lee, and Chang-Su Kim. Blind image quality assessment based on geometric order learning. In *Proceedings of the IEEE/CVF Conference on Computer Vision and Pattern Recognition*, pp. 12799–12808, 2024.

Suhas Srinath, Shankhanil Mitra, Shika Rao, and Rajiv Soundararajan. Learning generalizable perceptual representations for data-efficient no-reference image quality assessment. In *WACV*, pp. 22–31, 2024.

Shaolin Su, Qingsen Yan, Yu Zhu, Cheng Zhang, Xin Ge, Jinqiu Sun, and Yanning Zhang. Blindly assess image quality in the wild guided by a self-adaptive hyper network. In *CVPR*, pp. 3667–3676, 2020.

Quan Sun, Yuxin Fang, Ledell Wu, Xinlong Wang, and Yue Cao. Eva-clip: Improved training techniques for clip at scale. *arXiv preprint arXiv:2303.15389*, 2023.

Xiaoshuai Sun, Hongxun Yao, Rongrong Ji, and Shaohui Liu. Photo assessment based on computational visual attention model. In *ACM MM*, pp. 541–544, 2009.

Jianyi Wang, Kelvin CK Chan, and Chen Change Loy. Exploring clip for assessing the look and feel of images. In *AAAI*, volume 37, pp. 2555–2563, 2023.

Haoning Wu, Zicheng Zhang, Erli Zhang, Chaofeng Chen, Liang Liao, Annan Wang, Chunyi Li, Wenxiu Sun, Qiong Yan, Guangtao Zhai, et al. Q-bench: A benchmark for general-purpose foundation models on low-level vision. *arXiv preprint arXiv:2309.14181*, 2023a.

Haoning Wu, Zicheng Zhang, Weixia Zhang, Chaofeng Chen, Liang Liao, Chunyi Li, Yixuan Gao, Annan Wang, Erli Zhang, Wenxiu Sun, et al. Q-align: Teaching lmms for visual scoring via discrete text-defined levels. *arXiv preprint arXiv:2312.17090*, 2023b.

Kangmin Xu, Liang Liao, Jing Xiao, Chaofeng Chen, Haoning Wu, Qiong Yan, and Weisi Lin. Boosting image quality assessment through efficient transformer adaptation with local feature enhancement. In *Proceedings of the IEEE/CVF Conference on Computer Vision and Pattern Recognition*, pp. 2662–2672, 2024.

Sidi Yang, Tianhe Wu, Shuwei Shi, Shanshan Lao, Yuan Gong, Mingdeng Cao, Jiahao Wang, and Yujiu Yang. Maniqa: Multi-dimension attention network for no-reference image quality assessment. In *Proceedings of the IEEE/CVF Conference on Computer Vision and Pattern Recognition*, pp. 1191–1200, 2022.

Lewei Yao, Runhui Huang, Lu Hou, Guansong Lu, Minzhe Niu, Hang Xu, Xiaodan Liang, Zhenguo Li, Xin Jiang, and Chunjing Xu. Filip: Fine-grained interactive language-image pre-training. *arXiv preprint arXiv:2111.07783*, 2021.

Qinghao Ye, Haiyang Xu, Guohai Xu, Jiabo Ye, Ming Yan, Yiyang Zhou, Junyang Wang, Anwen Hu, Pengcheng Shi, Yaya Shi, et al. mplug-owl: Modularization empowers large language models with multimodality. *arXiv preprint arXiv:2304.14178*, 2023.

Ran Yi, Haoyuan Tian, Zhihao Gu, Yu-Kun Lai, and Paul L Rosin. Towards artistic image aesthetics assessment: a large-scale dataset and a new method. In *Proceedings of the IEEE/CVF Conference on Computer Vision and Pattern Recognition*, pp. 22388–22397, 2023.

Zhenqiang Ying, Haoran Niu, Praful Gupta, Dhruv Mahajan, Deepti Ghadiyaram, and Alan Bovik. From patches to pictures (paq-2-piq): Mapping the perceptual space of picture quality. In *CVPR*, pp. 3575–3585, 2020.

Jiahui Yu, Zirui Wang, Vijay Vasudevan, Legg Yeung, Mojtaba Seyedhosseini, and Yonghui Wu. Coca: Contrastive captioners are image-text foundation models. *arXiv preprint arXiv:2205.01917*, 2022.

Zihao Yu, Fengbin Guan, Yiting Lu, Xin Li, and Zhibo Chen. Sf-iqa: Quality and similarity integration for ai generated image quality assessment. In *Proceedings of the IEEE/CVF Conference on Computer Vision and Pattern Recognition*, pp. 6692–6701, 2024.

Guanghui Yue, Di Cheng, Tianwei Zhou, Jingwen Hou, Weide Liu, Long Xu, Tianfu Wang, and Jun Cheng. Perceptual quality assessment of enhanced colonoscopy images: A benchmark dataset and an objective method. *IEEE Transactions on Circuits and Systems for Video Technology*, 33 (10):5549–5561, 2023.

Kaiwei Zhang, Dandan Zhu, Xiongkuo Min, Zhongpai Gao, and Guangtao Zhai. Synergetic assessment of quality and aesthetic: Approach and comprehensive benchmark dataset. *IEEE TCSVT*, 2023a.

Lin Zhang, Lei Zhang, and Alan C Bovik. A feature-enriched completely blind image quality evaluator. *IEEE Transactions on Image Processing*, 24(8):2579–2591, 2015.

Weixia Zhang, Kede Ma, Jia Yan, Dexiang Deng, and Zhou Wang. Blind image quality assessment using a deep bilinear convolutional neural network. *IEEE TCSVT*, 30(1):36–47, 2018.

Weixia Zhang, Kede Ma, Guangtao Zhai, and Xiaokang Yang. Uncertainty-aware blind image quality assessment in the laboratory and wild. *IEEE TIP*, 30:3474–3486, 2021a.

Weixia Zhang, Guangtao Zhai, Ying Wei, Xiaokang Yang, and Kede Ma. Blind image quality assessment via vision-language correspondence: A multitask learning perspective. In *CVPR*, pp. 14071–14081, 2023b.

Xiaodan Zhang, Xinbo Gao, Wen Lu, Lihuo He, and Jie Li. Beyond vision: A multimodal recurrent attention convolutional neural network for unified image aesthetic prediction tasks. *IEEE TMM*, 23:611–623, 2020.

Xiaodan Zhang, Xinbo Gao, Lihuo He, and Wen Lu. Mscan: Multimodal self-and-collaborative attention network for image aesthetic prediction tasks. *Neurocomputing*, 430:14–23, 2021b.

Shiyu Zhao, Lin Zhang, Ying Shen, and Yicong Zhou. Refinednet: A weakly supervised refinement framework for single image dehazing. *IEEE Transactions on Image Processing*, 30:3391–3404, 2021.

Yan Zhong, Xingyu Wu, Li Zhang, Chenxi Yang, and Tingting Jiang. Causal-iqa: Towards the generalization of image quality assessment based on causal inference. In *Forty-first International Conference on Machine Learning*.

Ye Zhou, Xin Lu, Junping Zhang, and James Z Wang. Joint image and text representation for aesthetics analysis. In *ACM MM*, pp. 262–266, 2016.

Deyao Zhu, Jun Chen, Xiaoqian Shen, Xiang Li, and Mohamed Elhoseiny. Minigpt-4: Enhancing vision-language understanding with advanced large language models. *arXiv preprint arXiv:2304.10592*, 2023.

Hancheng Zhu, Leida Li, Jinjian Wu, Weisheng Dong, and Guangming Shi. Metaiqa: Deep meta-learning for no-reference image quality assessment. In *CVPR*, pp. 14143–14152, 2020.

Mengmeng Zhu, Guanqun Hou, Xinjia Chen, Jiaxing Xie, Haixian Lu, and Jun Che. Saliency-guided transformer network combined with local embedding for no-reference image quality assessment. In *ICCV*, pp. 1953–1962, 2021.

A MORE DISCUSSION AND DETAILS

A.1 DISCUSSION ABOUT THE AIR

We propose the Aesthetics-relevance and Informativeness Rank (AIR) to select the high-quality texts corresponding to an image. The AIR can be expressed as follows:

$$\mathrm{AIR} = \mathrm{Rank}((\mathrm{AR}^1 + \mathrm{IR}^1), \cdots, (\mathrm{AR}^n + \mathrm{IR}^n)). \tag{9}$$

where AR and IR denote the Aesthetics-relevance Rank and Informativeness Rank, respectively; n is the number of comments corresponding to an image. For simplicity, we directly take the summation of IR and AR to reflect the semantic relevance and richness of the text. In fact, we can introduce two factors (α and β) to purify the data more flexibly. Now, the modified AIR_m can be formulated as:

$$\mathrm{AIR}_\mathrm{m} = \mathrm{Rank}((\alpha\mathrm{AR}^1 + \beta\mathrm{IR}^1), \cdots, (\alpha\mathrm{AR}^n + \beta\mathrm{IR}^n)). \tag{10}$$

For instance, we can use large α for the highly noisy data. With this strategy, we can more flexibly purify data based on data quality.

Table 7: Details of different IQA datasets.

Dataset	Dataset Type	Dataset Size	Number of distortions
LIVE Sheikh et al. (2006)	Synthetic	799	5
CSIQ Larson & Chandler (2010)	Synthetic	866	5
TID2013 Ponomarenko et al. (2013)	Synthetic	3,000	24
KADID Lin et al. (2019)	Synthetic	10,125	25
CLIVE Ghadiyaram & Bovik (2015)	Authentic	1,162	-
KonIQ Hosu et al. (2020)	Authentic	10,073	-
SPAQ Fang et al. (2020)	Authentic	11,000	-
FLIVE Ying et al. (2020)	Authentic	39,810	-
AGIQA-3K Li et al. (2023b)	Authentic	2,982	-

Table 8: Results on LIVE dataset Sheikh et al. (2006). **Black** and **blue** numbers in bold represent the best and second best, respectively. Higher SRCC and PLCC imply better performance.

	LIVE	
Method	SRCC	PLCC
DIIVINE Bosse et al. (2017)	0.892	0.908
BRISQUE Mittal et al. (2012a)	0.929	0.944
ILNIQE Zhang et al. (2015)	0.902	0.906
BIECON Kim & Lee (2016)	0.958	0.961
MEON Ma et al. (2017)	0.951	0.955
WaDIQaM Bosse et al. (2017)	0.960	0.955
DBCNN Zhang et al. (2018)	0.968	0.971
MetaIQA Zhu et al. (2020)	0.960	0.959
PaQ-2-PiQ Ying et al. (2020)	0.959	0.958
HyperIQA Su et al. (2020)	0.962	0.966
TReS Golestaneh et al. (2022)	0.969	0.968
MUSIQ Ke et al. (2021)	0.940	0.911
DACNN Pan et al. (2022)	0.978	0.980
DEIQT Qin et al. (2023)	**0.980**	**0.982**
LIQE Zhang et al. (2023b)	0.970	0.951
Re-IQA (Saha et al., 2023)	0.970	0.971
LoDA (Xu et al., 2024)	0.975	0.979
Ours	**0.981**	**0.983**

A.2 DETAILS OF DATASETS AND EVALUATION CRITERIA

We list the details of the datasets used in our work in Table 7, including the dataset type, dataset size and number of distortion types. Since the distortions of authentic datasets are diverse, their number cannot be counted.

We employ Spearman's Rank-order Correlation Coefficient (SRCC) and Pearson's Linear Correlation Coefficient (PLCC) as criteria to measure the performance of IQA and IAA models. They reflect the prediction monotonicity and prediction accuracy of the model, respectively. Both SRCC and PLCC range from 0 to 1. Higher values of SRCC and PLCC indicate better performance.

Table 9: Training settings for different datasets.

Dataset	Task	Epoch	Batch size	Learning rate
LIVE Sheikh et al. (2006)	IQA	50	8	2e-4
CSIQ Larson & Chandler (2010)	IQA	50	8	2e-4
TID2013 Ponomarenko et al. (2013)	IQA	20	8	2e-4
KADID Lin et al. (2019)	IQA	20	8	2e-4
CLIVE Ghadiyaram & Bovik (2015)	IQA	50	8	2e-4
KonIQ Hosu et al. (2020)	IQA	20	8	2e-4
SPAQ Fang et al. (2020)	IQA	20	8	2e-4
AVA Murray et al. (2012)	IAA	20	128	5e-4
AADB Kong et al. (2016)	IAA	20	8	5e-4

A.3 More Implementation Details

For the pre-training, we employ the same training strategy as CLIP Radford et al. (2021) to pre-train our UniQA. The pre-training is resource-friendly and takes *less than an hour* at a time. When fine-tuning the adapter for downstream assessment tasks, we use different training settings according to the task and size of the dataset. Table 9 shows the detailed training setting for the different datasets. We follow the typical training strategy to fine-tune each dataset, including random cropping and random horizontal flipping. Since different datasets have different MOS scales, we scale their range to [0, 1] through normalization. During inference, we typically crop an input image into 10 image patches and take their average as the quality score of this image Su et al. (2020); Qin et al. (2023). We use the resolution of 224×224 for training and testing. All experiments are conducted on two A100 GPUs.

A.4 Prompt Ensemble

When applying our UniQA to zero-shot and few-label settings, prompt ensemble is a useful strategy to improve performance. Table 10 shows the prompt groups used in these two settings. Note that the prompts used in AGIQA-3K are different from other IQA datasets. This is because distortions in AIGC-generated images and authentic images tend to be different. For example, distortions in authentic images may come from camera shake. However, distortions in AIGC-generated images typically come from low-quality content, such as meaningless content and distorted poses. Therefore, we use "content" to prompt the pre-trained multimodal model for the AGIQA-3K dataset.

B More Experimental Results

B.1 Comparison Results on LIVE

Tab .8 shows the comparison results with other methods on LIVE dataset Sheikh et al. (2006). We can observe that our method also achieves state-of-the-art (SOTA) performance, verifying the effectiveness of our method.

B.2 More generalization experiments

In this section, we conduct more experiments to further verify the generalization capability of UniQA. We evaluate our model on three dataset, including AIGC IQA datatset AIGIQA-20K, the enhanced colonoscopy image quality assessment dataset (ECIQAD) and the AI-Generated Image Naturalness (AGIN) dataset.

AIGIQA-20K. AIGIQA-20K Li et al. (2024) is a large-scale AI-generated image quality assessment dataset. It consists of 20,000 images in total, with 14,000 images for training, 2,000 images for

Table 10: Text prompts used in zero-shot and few-label learning.

Task	Prompt
CLIVE, KonIQ, LIVE	{bad, poor, fair, good, perfect} with image
	{extremely blurry, blurry, fair, sharp, extremely sharp} with image
	{extremely noisy, noisy, fair, noise-free, extremely noise-free} with image
	{extremely low-quality, low-quality, fair, high-quality, extremely high-quality} with image
AGIQA-3K	{bad, poor, fair, good, perfect} with image {bad, poor, fair, good, perfect} with content

Table 11: Results on AIGIQA-20K dataset Li et al. (2024). * indicates that we also unfreeze the backbone for training with a smaller learning rate of 2e-6.

Method	SRCC	PLCC
CLIPIQA	0.331	0.483
CLIIQA+Finetune	0.786	0.712
CNNIQA	0.330	0.367
CNNIQA+Finetune	0.597	0.591
Q-Align	0.746	0.742
DBCNN Zhang et al. (2018)	0.471	0.512
DBCNN+Finetune	**0.851**	0.869
Ours	0.576	0.563
Ours+Finetune	0.830	**0.885**
Ours+Finetune*	**0.858**	**0.901**

validation, and 4,000 images for testing. We test our model on the zero-shot and fine-tuning setting. For fine-tuning, we use a learning rate of 2e-4 for the adapter and train the model for 10 epochs. As shown in Table 11, we can notice that our model achieves competitive results in both settings. These results verify the excellent generalization ability of UniQA on AI-generated images.

ECIQAD. ECIQAD (Yue et al., 2023) is an enhanced colonoscopy image quality assessment dataset containing 2400 images in total. We repeat the experiment 10 times with an 8:2 data split and report the median results. We train the model for 50 epochs. Other training settings are the same as AIGIQA-20K. The experimental results are shown in Table 12. Our method achieves SOTA results on ECIQAD. Since the ECIQAD dataset is quite different from natural images, these results fully demonstrate the strong generalization and image assessment capabilities of our method.

AGIN. AGIN (Chen et al., 2023) is an AI-Generated Image Naturalness (AGIN) dataset, which includes 6049 images. We randomly split the training, validation, and testing set into 7:1:2. We repeat this process 5 times and report the average performance as the final experimental results. We train the model for 20 epochs. As shown in Table 13, although our approach is not specifically designed for the AI naturalness problem, our method achieves competitive results compared to specific designed JOINT (Chen et al., 2023) and other methods. These results further demonstrate the generalization ability of our model.

B.3 PLCC Comparison in the Data-efficient Setting

The Pearson's Linear Correlation Coefficient (PLCC) comparisons for our method against other IQA methods corresponding to the table in the main paper are provided in Tab .14. We note that our method outperforms all other methods in terms of PLCC metric.

Table 12: Results on ECIQAD (Yue et al., 2023). * indicates that we also unfreeze the backbone for training with a smaller learning rate of 2e-6.

Method	SRCC	PLCC
BRISQUE (Mittal et al., 2012a)	0.436	0.459
BIQME (Gu et al., 2017)	0.770	0.768
BPRI (Min et al., 2017)	0.152	0.181
FRIQUEE (Ghadiyaram & Bovik, 2017)	0.663	0.656
CIQA (Chen et al., 2021)	0.738	0.735
ECIQ (Ke et al., 2021)	0.839	0.842
Ours	**0.873**	**0.887**
Ours*	**0.918**	**0.928**

Table 13: Results on AGIN (Chen et al., 2023). * indicates that we also unfreeze the backbone for training with a smaller learning rate of 2e-6.

Methods	Technical		Rationality		Naturalness	
	SRCC	PLCC	SRCC	PLCC	SRCC	PLCC
BRISQUE (Mittal et al., 2012a)	0.4867	0.4909	0.3608	0.3684	0.3745	0.4067
NIQE (Mittal et al., 2012b)	0.4235	0.4279	0.3144	0.3211	0.3358	0.3378
DBCNN (Zhang et al., 2018)	0.7623	0.7661	0.6834	0.6838	0.7057	0.7128
HyperIQA (Su et al., 2020)	0.7752	0.7806	0.7196	0.7292	0.7365	0.7509
MUSIQ (Ke et al., 2021)	0.7286	0.7355	0.6974	0.7013	0.7066	0.7103
UNIQUE (Zhang et al., 2021a)	0.7358	0.7434	0.6583	0.6685	0.6772	0.6789
MANIQA (Yang et al., 2022)	0.7763	0.7817	0.7192	0.7217	0.7385	0.7343
PAIAA (Li et al., 2020)	0.4763	0.4833	0.4532	0.4596	0.4483	0.4528
TANet (He et al., 2022)	0.5367	0.5587	0.4731	0.4762	0.4782	0.4535
Del. Transf. (He et al., 2023a)	0.5882	0.6134	0.5037	0.4942	0.4805	0.4961
SAAN (Yi et al., 2023)	0.4299	0.4380	0.4009	0.4160	0.4196	0.4184
JOINT (Chen et al., 2023)	**0.8173**	**0.8235**	0.7564	0.7711	0.7986	0.8028
JOINT++ (Chen et al., 2023)	**0.8351**	**0.8429**	**0.8033**	**0.8127**	**0.8264**	**0.8362**
Ours	0.7524	0.8007	0.7728	0.7793	0.7882	0.7979
Ours	0.7785	0.8104	**0.7898**	**0.7952**	**0.8069**	**0.8171**

B.4 More Comparison Results on IQA Datasets

To demonstrate the superiority of our method more comprehensively, we present more comparison results on the typical IQA datasets in Table 15.

B.5 More Results of Ablation Study

Table 16 shows the SRCC and PLCC results of the ablation study.

C Analysis of Constructed Multimodal Dataset

In this section, we analyze the constructed multimodal image and text dataset. Our proposed dataset has 273,897 images, with 1,240,915 captions. Next we conduct a detailed analysis of the dataset:

1. Firstly, we compare the data volume of the IQA and IAA datasets in Figure 6. IQA includes 39,807 images and IAA includes 234,090 images. We generate three captions for each IQA image and one caption for each IAA image, resulting 119,421 generated IQA captions and 234,090 IAA captions. From the ablation experiment in Table 6, we notice that Y_{IQA} and Y_{IAA} have similar performance improvements on the model, although Y_{IAA} has more data. Therefore, this shows that the text generated by MLLM tends to have the same structure and lacks diversity, limiting the further improvement of model performance.
2. Secondly, we analyze the number of words in the generated text, as shown in Figure 7. We can see that the number of words in most texts is between 20 and 40. In addition, there are

Table 14: PLCC performance comparison of our method with other NR-IQA methods trained using few labels. * denotes using ensemble prompts.

Method	LIVEC 50	LIVEC 100	LIVEC 200	KonIQ 50	KonIQ 100	KonIQ 200	LIVE 50	LIVE 100	LIVE 200
HyperIQA (Su et al., 2020)	0.689	0.755	0.806	0.650	0.758	0.807	0.903	0.922	0.931
TReS (Golestaneh et al., 2022)	0.702	0.776	0.813	0.740	0.748	0.824	0.916	**0.948**	**0.960**
ResNet50 (He et al., 2016)	0.580	0.629	0.660	0.661	0.693	0.716	0.872	0.908	0.920
CLIP (Radford et al., 2021)	0.676	0.739	0.758	0.749	0.790	0.802	0.891	0.924	0.942
CONTRIQUE (Madhusudana et al., 2022)	0.693	0.736	0.777	0.743	0.801	0.832	0.892	0.922	0.944
CLIPIQA (Wang et al., 2023)	0.633	0.606	0.639	0.586	0.616	0.681	0.613	0.706	0.752
Re-IQA (Saha et al., 2023)	0.620	0.650	0.701	0.689	0.693	0.757	0.876	0.892	0.931
DEIQT (Qin et al., 2023)	0.695	0.739	0.818	0.670	0.707	0.778	0.916	0.942	0.957
GRepQ (Srinath et al., 2024)	**0.772**	**0.798**	**0.835**	**0.793**	**0.816**	**0.840**	**0.929**	0.936	0.957
Ours	0.819	0.854	0.866	0.815	0.861	0.890	0.952	0.959	0.970
Ours*	**0.826**	**0.847**	**0.869**	**0.857**	**0.883**	**0.893**	**0.963**	**0.962**	**0.973**

Table 15: Results on IQA datasets. **Black** and **blue** numbers in bold represent the best and second best, respectively. Higher SRCC and PLCC imply better performance.

Method	TID2013 SRCC	TID2013 PLCC	CSIQ SRCC	CSIQ PLCC	KADID SRCC	KADID PLCC	CLIVE SRCC	CLIVE PLCC	KonIQ SRCC	KonIQ PLCC	SPAQ SRCC	SPAQ PLCC
DIIVINE Bosse et al. (2017)	0.643	0.567	0.804	0.776	0.413	0.435	0.588	0.591	0.546	0.558	0.599	0.600
BRISQUE Mittal et al. (2012a)	0.626	0.571	0.812	0.748	0.528	0.567	0.629	0.629	0.681	0.685	0.809	0.817
ILNIQE Zhang et al. (2015)	0.521	0.648	0.822	0.865	0.534	0.558	0.508	0.508	0.523	0.537	0.712	0.713
BIECON Kim & Lee (2016)	0.717	0.762	0.815	0.823	0.623	0.648	0.613	0.613	0.651	0.654	-	-
MEON Ma et al. (2017)	0.808	0.824	0.852	0.864	0.604	0.691	0.697	0.710	0.611	0.628	-	-
WaDIQaM Bosse et al. (2017)	0.835	0.855	0.852	0.844	0.739	0.752	0.682	0.671	0.804	0.807	0.840	0.845
DBCNN Zhang et al. (2018)	0.816	0.865	0.946	0.959	0.851	0.856	0.851	0.869	0.875	0.884	0.911	0.915
MetaIQA Zhu et al. (2020)	0.856	0.868	0.899	0.908	0.762	0.775	0.802	0.835	0.850	0.887	-	-
PaQ-2-PiQ Ying et al. (2020)	0.862	0.856	0.899	0.902	0.840	0.849	0.844	0.842	0.872	0.885	-	-
HyperIQA Su et al. (2020)	0.840	0.858	0.923	0.942	0.852	0.845	0.859	0.882	0.906	0.917	0.911	0.915
TReS Golestaneh et al. (2022)	0.863	0.883	0.922	0.942	0.859	0.858	0.846	0.877	0.915	0.928	-	-
MUSIQ Ke et al. (2021)	0.773	0.815	0.871	0.893	0.875	0.872	0.702	0.746	0.916	0.928	0.918	0.921
DACNN (Pan et al., 2022)	0.871	0.889	0.943	0.957	0.905	0.905	0.866	0.884	0.901	0.912	0.915	0.921
DEIQT (Qin et al., 2023)	**0.892**	**0.908**	0.946	**0.963**	0.889	0.887	0.875	0.894	0.921	0.934	0.919	0.923
LIQE (Zhang et al., 2023b)	-		0.936	0.939	0.930	0.931	**0.904**	**0.911**	0.919	0.908	-	-
Re-IQA (Saha et al., 2023)	0.804	0.861	**0.947**	0.960	0.872	0.885	0.840	0.854	0.914	0.923	0.918	0.925
CIS (Zhong et al.)	-	-	-	-	-	-	0.828	0.847	0.881	0.918	-	-
LAR-IQA Avanaki et al. (2024)	-	-	-	-	**0.941**	**0.965**	-	-	-	-		
LoDA (Xu et al., 2024)	0.869	0.901	-	-	0.931	0.936	0.876	0.899	0.932	**0.944**	**0.925**	0.928
DP-IQA Fu et al. (2024)	-	-	-	-	-	-	0.893	0.913	**0.942**	**0.951**	0.923	0.926
Q-Align (Wu et al., 2023b)	-	-	0.915	0.936	0.869	0.927	**0.931**	**0.921**	**0.935**	0.934	-	-
Ours	**0.916**	**0.931**	**0.963**	**0.973**	**0.940**	**0.943**	0.890	0.905	0.933	0.941	**0.924**	**0.928**

also many samples with the number of words between 80-120, which are texts generated by MLLM.

3. Finally, we construct a word cloud for the text data, as shown in Figure 8. It can be seen that the most common words in the text dataset are aesthetic and quality-related words, such as "aesthetics", "quality", "composition", "fair", etc. This indicates that the text of the constructed dataset focuses on image assessment.

D Details and Discussion of MLLMs Captioning

Details of MLLMs Captioning. We use different numbers of captions for IQA and IAA tasks. Considering that the IQA data does not have textual descriptions, we generate three captions with different prompts via MLLMs for the IQA datasets. This method can improve the text diversity of IQA image-text data. For the IAA dataset, we generate one caption for each image because IAA datasets have a large amount of authentic text data. Details of the prompts for quality-related captioning are shown in Figure 9.

Effectiveness of text guidance. We visualize the MLLMs-generated captions with/without text guidance to evaluate the effectiveness of text guidance. We take the captioning for IQA datasets as examples. As shown in Figure 13, when the quality of image is high, the MLLMs can output correct caption (see example 1). *However, we can observe that the MLLMs will generate wrong captions*

Table 16: Ablation experiments on two IQA datasets (CLIVE and KonIQ) and one IAA dataset (AVA). Different ablations are distinguished by different backgrounds for better viewing.

	CLIVE		KonIQ		AVA	
Ablation type	SRCC	PLCC	SRCC	PLCC	SRCC	PLCC
Ablation on different pre-training data						
Y_{IQA} Y_{IAA} Y^{+}_{IAA}						
× × ×	0.865	0.886	0.907	0.924	0.748	0.747
✓ × ×	0.871	0.898	0.914	0.932	0.755	0.755
× ✓ ×	0.871	0.895	0.917	0.932	0.755	0.756
✓ ✓ ×	0.874	0.892	0.918	0.932	0.756	0.757
× × ✓	0.875	0.895	0.928	0.937	0.773	0.774
× ✓ ✓	0.877	0.895	0.930	0.939	0.774	0.774
✓ ✓ ✓	**0.890**	**0.905**	**0.933**	**0.941**	**0.776**	**0.776**
Ablation on data purification strategy						
w/o Strategy	0.876	0.899	0.929	0.940	0.772	0.771
IR Strategy	0.879	0.898	0.931	0.941	0.774	0.774
AR Strategy	0.885	0.901	0.930	0.942	0.774	0.773
AIR Strategy	**0.890**	**0.905**	**0.933**	**0.941**	**0.776**	**0.776**
Ablation on the proposed adapter						
Single Prompt	0.705	0.720	0.920	0.931	0.765	0.765
Antonym Prompt	0.875	0.897	0.928	0.938	0.771	0.772
Ours adapter	**0.890**	**0.905**	**0.933**	**0.941**	**0.776**	**0.776**
Ablation on different MLLMs						
LLaVA-v1.5-7B	0.871	0.898	0.914	0.932	0.755	0.755
LLaVA-v1.5-13B	0.872	0.897	0.914	0.929	0.757	0.759
Sphinx	0.874	0.902	0.916	0.931	0.758	0.758
QWen-VL	0.870	0.895	0.913	0.930	0.757	0.758
LLaVa-7B+QWen	0.875	0.899	0.916	0.930	0.758	0.757
Sphinx+QWen	**0.877**	**0.908**	**0.918**	**0.934**	**0.759**	**0.760**

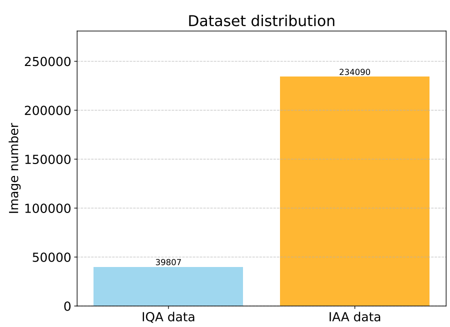

Figure 6: The number of images for the two tasks in the constructed dataset.

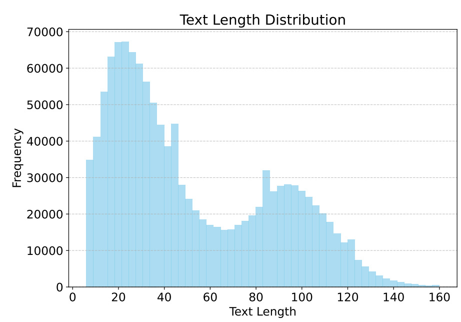

Figure 7: The length distribution of texts in the dataset.

when low-quality images are sent to MLLMs and the text guidance is not provided (see example 2-4 of Figure 13). As a result, the text guidance is useful and necessary for MLLMs captioning.

E More visualization

E.1 More Examples of Zero-shot Retrieval

We show more examples of zero-shot retrieval in Figure 10, Figure 11 and Figure 12. We explore the model's retrieval capabilities in terms of color and light. We can observe that the images of "Good color" show harmonious and vivid colors while the images of "Bad color" present messy

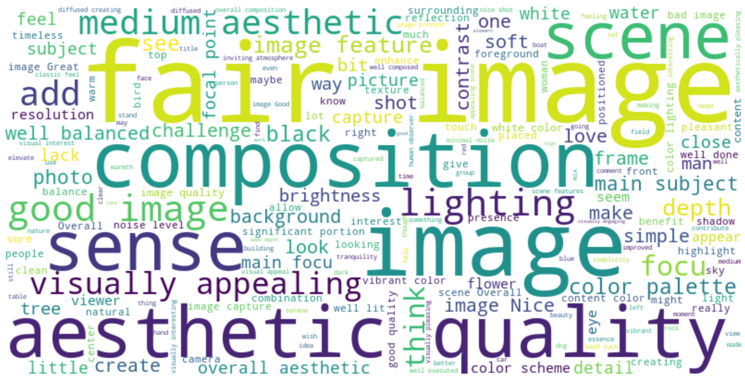

Figure 8: Word cloud of the constructed dataset.

Details of quality-related captioning

MOS of image: 6.71 → **Text level**: good

Instruction 1: What you are given is a good quality image. Evaluate image quality based on factors such as *sharpness, color balance, and noise levels.*

Output 1: The image is of three hot air balloons flying in the sky. The balloons are of different sizes and are positioned at various heights. The sky is clear and blue, providing a perfect backdrop for the balloons. The resolution of the image is good, allowing for clear visibility of the balloons and their details. Overall, the image quality is excellent, capturing the essence of the hot air balloons in flight.

Instruction 2: Giving you a good quality image. Describe the quality of an image based on visual descriptors such as *resolution, noise, brightness*.

Output 2: The image is of good quality, with a resolution that allows for clear visibility of the three hot air balloons flying in the sky. The noise level is low, and the brightness of the scene is well-balanced, making it an enjoyable view. Overall, the image is high quality and has clear content.

Instruction 3: This is a good quality (*sharpness, contrast, distortion*) image. Assuming you are a human observer, please describe your feelings when you see this image.

Output 2: As a human observer, I would feel a sense of wonder and excitement upon seeing this image. The two hot air balloons flying in the sky, each with a unique design, create a visually appealing and captivating scene. The contrast between the vibrant colors of the balloons and the clear blue sky adds to the overall beauty of the image.

Figure 9: Details of the prompts of quality-related captioning. We generate three captions for each IQA image using three different prompts.

colors. For the retrieval on light, the images of "Good light" are clear and well-lit and the images of "Bad light" demonstrate dimly lit environments and poor lighting. These visualization results further demonstrate the strong capability of our model in understanding concepts related to quality and aesthetics.

E.2 Visualization of Data Purification Strategy

In Figure 14, we visualize the comments sorted by the proposed strategies. As observed, the Aesthetics-relevance Rank (AR) can sort the aesthetics-related comments first. Further integrating the Informativeness Rank (IR), we can obtain aesthetically relevant comments with rich semantics.

E.3 More Examples of Text Generated by MLLMs

In Figure 15, we show more examples of the captions generated by MLLMs. We can observe that with our prompt design, MLLMs can output correct fine-grained quality- and aesthetics-related descriptions.

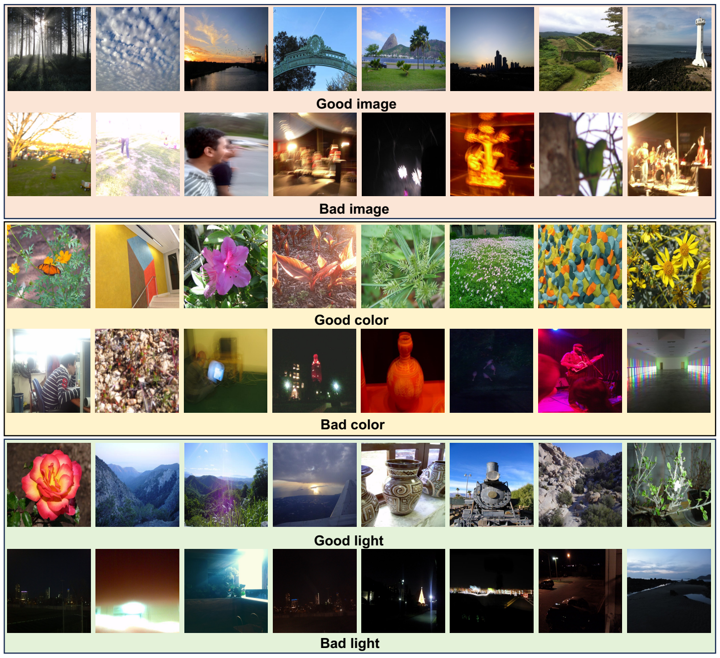

Figure 10: More image retrieval results with various text as queries on CLIVE Ghadiyaram & Bovik (2015).

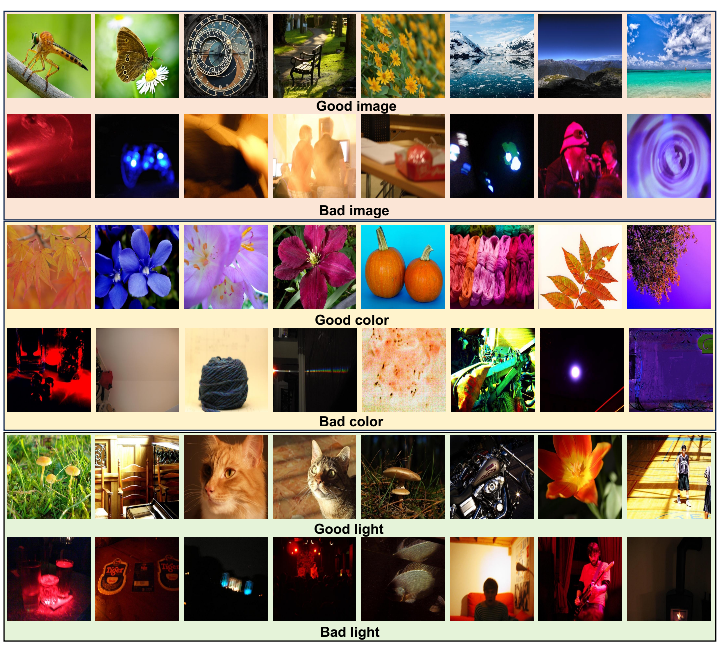

Figure 11: More image retrieval results with various text as queries on KonIQ Hosu et al. (2020).

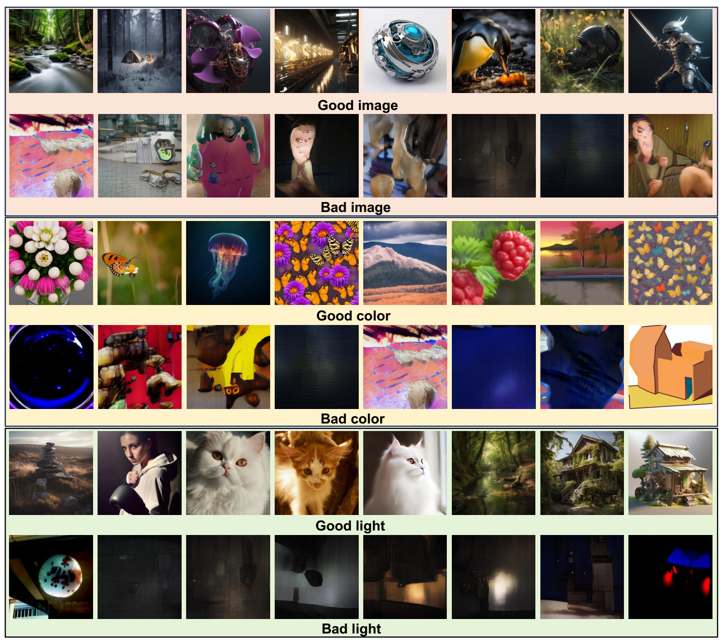

Figure 12: More image retrieval results with various text as queries on AGIQA-3K Li et al. (2023b).

Example 1

Captioning with MOS-based text guidance

MOS of image: 8.82 → **Text level**: perfect

Instruction: What you are given is a excellent quality image. Evaluate image quality based on factors such as *sharpness, color balance, and noise level*.

Output: The image of the silver Canon camera is of high quality. The noise is minimal, and the brightness is well-balanced, making it an excellent representation of the camera. The composition of the image is well-executed, with the camera being the main focus, and the background is clean and uncluttered. Overall, the image showcases the camera's features and design effectively.

Captioning without MOS-based text guidance

Instruction: Evaluate image aesthetics based on factors such as *content, color, lighting, and composition*.

Output: The image quality of the silver digital camera is quite good. The camera appears to be sharp, with clear details visible in the image. The color balance is also well-maintained, with vibrant colors and accurate representation of the scene. Overall, the image quality of the camera is impressive, making it suitable for capturing high-quality photos and videos.

Example 2

Captioning with MOS-based text guidance

MOS of image: 3.91 → **Text level**: bad

Instruction: What you are given is a bad quality image. Evaluate image quality based on factors such as *sharpness, color balance, and noise level*.

Output: The camera appears to be in focus, but the overall quality of the image is poor. The brightness of the image is also low, which further contributes to the poor quality. The composition of the image is simple, with the camera being the main subject, and there are no other objects or elements in the frame.

Captioning without MOS-based text guidance

Instruction: Evaluate image aesthetics based on factors such as *content, color, lighting, and composition*.

Output: The camera appears to be in good condition, with no visible signs of damage or wear. The image quality seems to be quite good, as the camera appears to be sharp and well-focused. The color balance appears to be accurate, with no noticeable color distortions or over-saturation. Overall, the image quality seems to be quite good, with a well-focused, accurate color balance, and minimal noise.

Example 3

Captioning with MOS-based text guidance

MOS of image: 3.65 → **Text level**: bad

Instruction: What you are given is a bad quality image. Evaluate image quality based on factors such as *sharpness, color balance, and noise level*.

Output: The image quality is poor, with a low resolution that makes it difficult to discern details. The brightness of the image is also low, making it challenging to see the subject clearly. The composition of the image is somewhat interesting, featuring a Chinese-style roof structure with a sign on it, but the overall quality of the image is not satisfactory.

Captioning without MOS-based text guidance

Instruction: Evaluate image aesthetics based on factors such as *content, color, lighting, and composition*.

Output: The image quality appears to be quite good, with a sharp focus on the yellow and white sign. The colors in the image are well-balanced, and there is minimal noise, making it a visually appealing scene. The night sky in the background adds a sense of depth and contrast to the image, further enhancing its overall quality.

Example 4

Captioning with MOS-based text guidance

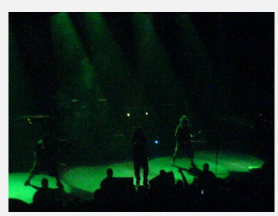

MOS of image: 1.01 → **Text level**: poor

Instruction: What you are given is a poor quality image. Evaluate image quality based on factors such as *sharpness, color balance, and noise level*.

Output: The image is of a concert with a group of people on stage. The resolution is low, which makes it difficult to discern the details of the performers and the audience. The brightness of the image is also low, making it hard to see the performers and the audience clearly. Overall, the image quality is poor due to low resolution, high noise, low brightness, and an unbalanced composition.

Captioning without MOS-based text guidance

Instruction: Evaluate image aesthetics based on factors such as *content, color, lighting, and composition*.

Output: The image quality appears to be quite good, with a high level of sharpness, color balance, and minimal noise. The image is a black and white photo of a band performing on stage, and the band members are clearly visible. The lighting in the scene is green, which adds a unique atmosphere to the image. Overall, the photo captures the essence of the live performance and the audience's engagement with the band.

Figure 13: Example of captioning with/without text guidance. The red text refers to MOS-based text guidance. The orange text highlights the correct quality-related caption. The green text indicates the incorrect quality-related caption without text guidance.

The Image

1. I really like this photo. I love the see-through globe. I like that the colours are so close to the ones used in the map below. It's a great composition.
2. Cool idea. I think the constellations should have been the focal point, and blur the earth globe a little bit. But great idea!
3. use a polarizer next time to get rid of the reflection... or wait.. I hear they don't work on plastic.
4. I can undesrtand it as a zodiac shoot. Perhaps I know so much about it.
5. Cool. how did it look with the constellations being the focus?
6. Nice composition, DOF is about perfect, good color. Nice job!
7. Not sure this meets the challenge.
8. Thanks for all your coments!
9. Creative.

(1) IR strategy

1. I really like this photo. I love the see-through globe. I like that the colours are so close to the ones used in the map below. It's a great composition.
2. Cool idea. I think the constellations should have been the focal point, and blur the earth globe a little bit. But great idea!
3. Cool. how did it look with the constellations being the focus?
4. Nice composition, DOF is about perfect, good color. Nice job!
5. I can undesrtand it as a zodiac shoot. Perhaps I know so much about it.
6. use a polarizer next time to get rid of the reflection... or wait.. I hear they don't work on plastic.
7. Thanks for all your coments!
8. Creative.
9. Not sure this meets the challenge.

(2) AR strategy

1. I really like this photo. I love the see-through globe. I like that the colours are so close to the ones used in the map below. It's a great composition.
2. Cool idea. I think the constellations should have been the focal point, and blur the earth globe a little bit. But great idea!
3. Cool. how did it look with the constellations being the focus?
4. I can undesrtand it as a zodiac shoot. Perhaps I know so much about it.
5. use a polarizer next time to get rid of the reflection... or wait.. I hear they don't work on plastic.
6. Nice composition, DOF is about perfect, good color. Nice job!
7. Thanks for all your coments!
8. Not sure this meets the challenge.
9. Creative.

(3) AIR strategy

The Image

1. Ok, I have looked at this long and hard, even asked my wife and both of us could not figure any connection with the zodiac. So tell me what it is.. huh?
2. I like the sharp detail of the bare tree, but the background looks very unnatural and the frame seems too heavy for the picture.
3. I am still trying to relate to the challenge... Not quite sure... But the picture itself is beautiful! Nice tones.
4. I'm not sure how this relates to the challenge. I don't dislike this shot..in fact the colors are very appealing.
5. Nice picture, very artistic and postcard like, but I fail to see who does it meet the challenge.
6. Which zodiac sign is the tree? Nice picture but I don't see how it fits the challenge.
7. Love the dark sepia, but missing the Zodiac.
8. Love the composition, color, and exposure.
9. What symbol is this for?
10. zodiac?

(1) IR strategy

1. I am still trying to relate to the challenge... Not quite sure... But the picture itself is beautiful! Nice tones.
2. Love the dark sepia, but missing the Zodiac.
3. I like the sharp detail of the bare tree, but the background looks very unnatural and the frame seems too heavy for the picture.
4. Nice picture, very artistic and postcard like, but I fail to see who does it meet the challenge.
5. Which zodiac sign is the tree? Nice picture but I don't see how it fits the challenge.
6. Love the composition, color, and exposure.
7. I'm not sure how this relates to the challenge. I don't dislike this shot..in fact the colors are very appealing.
8. Ok, I have looked at this long and hard, even asked my wife and both of us could not figure any connection with the zodiac. So tell me what it is.. huh?
9. zodiac?
10. What symbol is this for?

(2) AR strategy

1. I am still trying to relate to the challenge... Not quite sure... But the picture itself is beautiful! Nice tones.
2. I like the sharp detail of the bare tree, but the background looks very unnatural and the frame seems too heavy for the picture.
3. Love the dark sepia, but missing the Zodiac.
4. Nice picture, very artistic and postcard like, but I fail to see who does it meet the challenge.
5. Ok, I have looked at this long and hard, even asked my wife and both of us could not figure any connection with the zodiac. So tell me what it is.. huh?
6. I'm not sure how this relates to the challenge. I don't dislike this shot..in fact the colors are very appealing.
7. Which zodiac sign is the tree? Nice picture but I don't see how it fits the challenge.
8. Love the composition, color, and exposure.
9. zodiac?
10. What symbol is this for?

(3) AIR strategy

Figure 14: The comments sorted using different strategies. With our proposed strategy, we can obtain aesthetically relevant and informative comments. The order of comments is determined by the corresponding strategy. Gray sentences indicate being filtered.

Quality-related captioning

MOS of image: 7.21 → **Text level**: good
Instruction: Giving you a good quality image. Describe the quality of an image based on visual descriptors such as *resolution, noise, brightness*.
Output: The image is of a green and yellow parrot sitting on a wooden perch. The bird appears to be looking at the camera, and its vibrant colors make it stand out in the scene. The image is well-lit, with good contrast and resolution, allowing for a clear view of the parrot's features.

MOS of image: 7.80 → **Text level**: good
Instruction: What you are given is a good quality image. Evaluate image quality based on factors such as *sharpness, color balance, and noise levels*.
Output: The image of the elephant in the grassy field is of good quality. The resolution is high, allowing for clear details of the elephant's features, such as its tusks and trunk. The noise level is low, resulting in a clean and unobstructed view of the elephant. Overall, the image quality is excellent, making it an appealing representation of the elephant in its natural habitat.

MOS of image: 2.73 → **Text level**: bad
Instruction: Giving you a bad quality image. Describe the quality of an image based on visual descriptors such as *resolution, noise, brightness*.
Output: The image quality is poor, with a low resolution that makes it difficult to discern details. The brightness is low, making it hard to see the pumpkin clearly. The noise in the image is high, which adds to the overall poor quality.

Aesthetics-related captioning

MOS of image: 5.09 → **Text level**: fair
Instruction: What you get is an image of fair aesthetics. Evaluate image aesthetics based on factors such as *content, color, lighting, and composition*.
Output: The image presents a visually appealing scene with a combination of content, color, lighting, and composition. The sunset in the background creates a warm and serene atmosphere. The combination of these elements results in an aesthetically pleasing image that captures the viewer's attention and evokes a sense of tranquility.

MOS of image: 3.05 → **Text level**: bad
Instruction: What you get is an image of bad aesthetics. Evaluate image aesthetics based on factors such as *content, color, lighting, and composition*.
Output: In the image, there is a house with a lit-up Christmas tree in front of it. However, the overall aesthetics of the image are not appealing due to a few factors. Firstly, the tree is positioned in the foreground, occupying a significant portion of the frame, which can make the image feel cramped and cluttered. Secondly, the tree's lights are not evenly distributed, with some areas appearing brighter than others. This uneven lighting can create an unbalanced and unappealing visual effect.

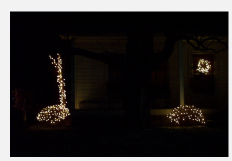

MOS of image: 8.04 → **Text level**: perfect
Instruction: What you get is an image of excellent aesthetics. Evaluate image aesthetics based on factors such as *content, color, lighting, and composition*.
Output: The image showcases an aesthetically pleasing scene of a lone tree standing in the middle of a grassy field at night. The tree is illuminated by the moonlight, creating a serene and peaceful atmosphere. The night sky is filled with stars, adding to the beauty and tranquility of the scene. The composition of the image, with the tree as the focal point, draws the viewer's attention and invites them to appreciate the natural beauty of the landscape. Overall, the image is visually appealing due to its content, color, lighting, and composition.

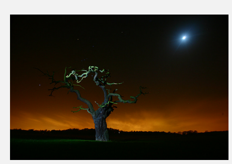

Figure 15: More examples of quality- and aesthetics-related captioning via MLLMs. The red text refers to MOS-based text guidance. The orange text highlights the quality- and aesthetics-related text.